CIV102 – Structures and Materials
An Introduction to Engineering Design
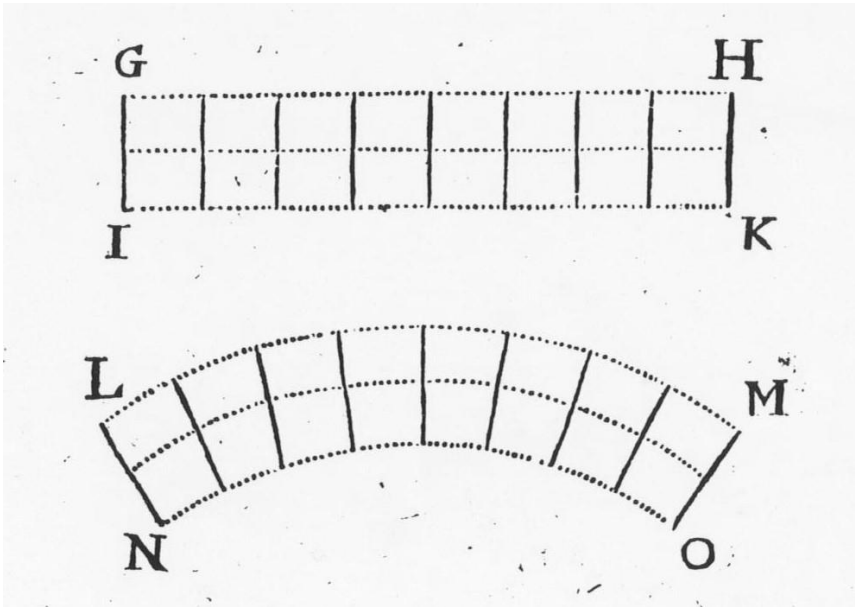
Part 3: Flexural Members – Beams and Box Girders

University of Toronto
Division of Engineering Science
September 2020

Allan Kuan
Michael P. Collins

Schematic of "Plane Sections Remain Plane", the fundamental assumption used in beam theory.

CIV102 Course Notes – Part 3: Flexural Members – Beams and Box Girders

Lecture 20 – Bending of Beams – Navier's Equation – 1826

Overview:
In this chapter, the derivation of Navier's equation for calculating the stresses in a beam caused by bending is presented. Relevant section properties are discussed, and the table of standard steel wide flange sections is explained.

Derivation of Navier's Equation
As previously discussed in Lecture 10, when a member is subjected to pure bending by applying a moment to its two ends, it curves to form the arc of a circle. If vertical lines were drawn on the member which are perpendicular to its longitudinal axis, these lines would remain straight as the member curves and point towards a common point. The assumption that those vertical lines – also referred to as plane sections – stay straight is known as the *plane sections remain plane* assumption. In Lecture 10, we concluded that this assumption results in the following equation for the longitudinal strain in the member, ε, which varies linearly over the height of the member:

$$\varepsilon(y) = \phi y \tag{20.1}$$

Fig. 20.1 – Bust of Claude-Louis Navier, who made many important contributions to the fields of elasticity and structural mechanics.

In Eq. (20.1), ϕ is the curvature in rad/mm and **y** is the vertical distance from the location of interest and the neutral axis of the member. The curvature is a measure of how curved a member is, being defined as the change in the member's slope per unit length, and the neutral axis is the location on the beam which does not experience any change in length as the member bends. These terms are defined in Fig. 20.2.

For a beam made from a linear elastic material, the stress will be related to the strain by the Young's modulus, **E**. Applying Hooke's law to Eq. (20.1) results in the following equation for the stress, which also varies linearly over the height:

$$\sigma(y) = E\phi y \tag{20.2}$$

Consider a differentially small area of the cross section, dA, which is located a distance **y** away from the neutral axis. The stress which it is carrying, $\sigma(y)$, will result in a differential force **dF(y)** acting through its centroid, which is calculated as:

$$dF(y) = \sigma(y)dA \tag{20.3}$$

This force will also produce a moment about the neutral axis, **dM(y)**:

$$dM(y) = ydF(y) = y\sigma(y)dA \tag{20.4}$$

Eq. (20.3) and (20.4) can be written in terms of the curvature and Young's modulus by using Eq. (20.2), which results in the following:

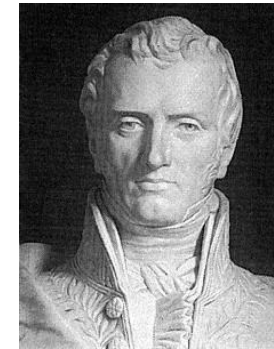$$dF(y) = E\phi y dA \tag{20.5}$$
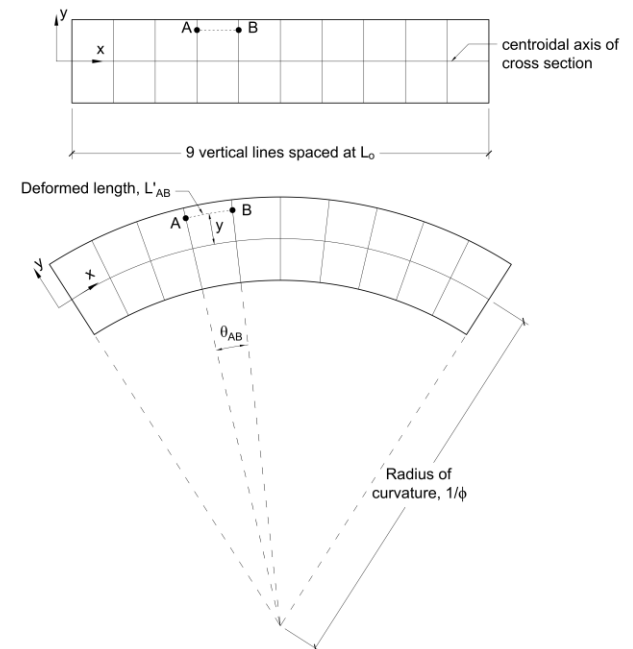
$$dM(y) = E\phi y^2 dA \tag{20.6}$$

Fig. 20.2 – Figure illustrating Robert Hooke's 1678 hypothesis that when members are subjected to pure bending, "Plane Sections Remain Plane". Reproduced from Fig. 10.1.

Integrating **dF** over the cross-sectional area produces the axial force, **N**, which is carried by the member. When subjected to pure bending, the axial force will be equal to zero, which results in the following equation:

$$N = \int_A E\phi y \, dA = 0 \tag{20.7}$$

In Eq. (20.7), the ϕ is a property of the member and **E** is a constant related to the material; if the member is homogeneous, neither of these quantities will vary over the cross section, and hence they can be removed from the integral. The resulting equation governs the location of the neutral axis when the member is subjected to pure bending, requiring that the ***first moment of area*** taken about the neutral, or centroidal, axis of the member equals zero.

$$0 = \int_A y \, dA \tag{20.8}$$

If we integrate **dM** in Eq. (20.6) over the cross-sectional area, we will obtain the bending moment which is carried by the member, **M**:

$$M = \int_A E\phi y^2 \, dA \tag{20.9}$$

We can evaluate Eq. (20.9) by first removing **E** and ϕ from the equation like we did to obtain Eq. (20.8). The resulting equation, which we derived in Lecture 10, contains an integral term, the ***second moment of area*** of the cross section, which is abbreviated as **I**:

$$M = E\phi \int_A y^2 \, dA = EI\phi \tag{20.10}$$

Eq. (20.10) illustrates the fundamental relationship between the bending moment carried by a member, **M**, and the curvature, ϕ. Combining Eq. (20.10) with Eq. (20.2) results in another important equation, which is the relationship between the moment and the flexural stresses in the member:

$$\sigma(y) = \frac{My}{I} \tag{20.11}$$

Eq. (20.11) is called ***Navier's Equation***, which allows the flexural stresses in a member with second moment of area, **I**, and carrying a bending moment, **M**, to be calculated. The resulting distribution of flexural stresses caused by bending moments is shown in Fig. 20.3, and a summary of the derivation is shown in Fig. 20.4.
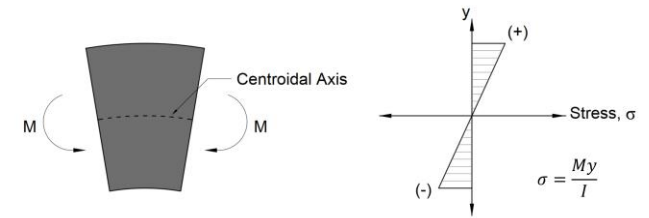

Fig. 20.3 – Distribution of flexural stresses caused by bending moments

Note: The relationship M = EIϕ was previously derived in Lecture 10.
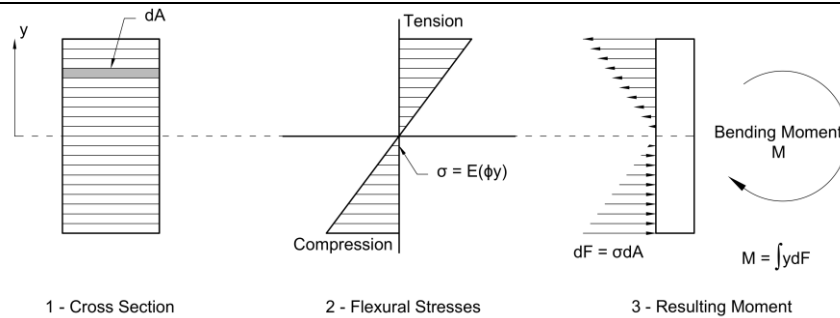
Fig. 20.4 – Summary of how the bending moment carried by a member is determined if the distribution of strains is known from the curvature. Reproduced from Fig. 10.3.

Fig. 20.5 – Steel wide flange beam cross section

Steel Wide Flange Members

A common type of member used in beams and columns in structures is called a ***wide flange section.*** Wide flange sections are commonly used in members which bend, like in beams, because their shape allows them to carry bending moments very efficiently. The reason for this is because most of their area is concentrated in the flanges, which are located far away from the centroidal axis, which is located at mid-height. Because the second moment of area is calculated by multiplying the area by the square of the distance from the centroidal axis, moving the area away from the neutral axis allows their contribution to **I** to be maximized.

Note: Wide-flange sections are often called I-beams when used as beams in buildings and bridges. When inserted into the ground to support structures built above, they are sometimes called H-piles.

Navier's equation states that the bending stresses vary linearly over the height of the member and are equal to zero at the location of the neutral axis. Because the maximum tensile and compressive stresses occur at the extremities of the member, it is often convenient to simply calculate the stresses on the top and bottom of the beam only. If we define y_{top} and y_{bot} as the vertical distance from the neutral axis to the top and bottom of the member respectively, then the largest flexural stresses can be found using the following equations:

$$\sigma_{max,top} = \frac{My_{top}}{I} = \frac{M}{S_{top}} \tag{20.12}$$

$$\sigma_{max,bot} = \frac{My_{bot}}{I} = \frac{M}{S_{bot}} \tag{20.13}$$

In Eq. (20.12) and (20.13), **S** is called the ***section modulus*** and allows the largest flexural stresses at the top and bottom of the member to be calculated in a concise manner. For members having a horizontal axis of symmetry, S_{top} and S_{bot} are the same.

Tables 20.1 and 20.2 show the section properties for common types of steel wide-flange sections and sawn timber sections respectively. The relevant properties for bending, **I**, **S** and the radius of gyration **r**, are specified for both the strong axis (x-x) and weak axis (y-y). The strong axis of bending, which refers to the orientation when the flanges of an I-beam are parallel to the centroidal axis, or when the taller dimension for a timber section is the height, typically has substantially higher values of **I**, **S** and **r** compared to when the member is oriented along its weak axis.
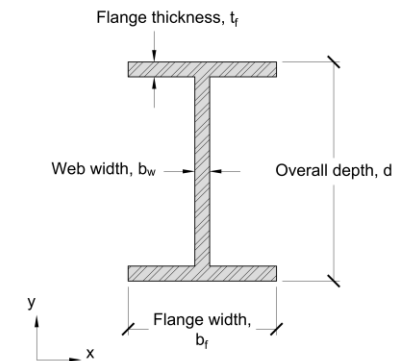
Note: Recall that the radius of gyration is defined as:

$$r = \sqrt{\frac{I}{A}}$$

Table 20.1 – Steel Wide Flange Beam Table

Note: The Torsion Constant will not be used in CIV102. The Shear Depth will be discussed when shear stresses are introduced in Lecture 25.

Wide Flange Rolled Steel Beams
Dimensions and Section Properties

Designation	Dimensions				Dead Load	Area	Strong Axis x-x			Weak Axis y-y			Torsion Constant	Shear Depth
	d	b_f	t	b_w			I_x	S_x	r_x	I_y	S_y	r_y	J	I_x/Q
mm × kg/m	mm	mm	mm	mm	kN/m	mm²	10^6 mm⁴	10^3 mm³	mm	10^6 mm⁴	10^3 mm³	mm	10^3 mm⁴	mm
W920 × 446	933	423	43	24.0	4.38	57000	8470	18200	385	540	2550	97.3	26800	822
× 365	916	419	34	20.3	3.57	46400	6710	14600	380	421	2010	95.3	14400	813
× 313	932	309	34	21.1	3.06	39800	5480	11800	371	170	1100	65.4	11600	806
× 238	915	305	26	16.5	2.33	30400	4060	8880	365	123	806	63.6	5140	796
W840 × 329	862	401	32	19.7	3.23	42000	5350	12400	357	349	1740	91.2	11500	764
× 210	846	293	24	15.4	2.06	26800	3110	7340	341	103	700	62.0	4050	738
× 176	835	292	19	14.0	1.72	22400	2460	5900	331	78.2	536	59.1	2220	722
W760 × 257	773	381	27	16.6	2.52	32800	3420	8840	323	250	1310	87.3	6380	689
× 173	762	267	22	14.4	1.70	22100	2060	5400	305	68.7	515	55.8	2690	663
× 147	753	265	17	13.2	1.44	18700	1660	4410	298	52.9	399	53.2	1560	651
W690 × 217	695	355	25	15.4	2.13	27700	2340	6740	291	185	1040	81.7	4560	618
× 152	688	254	21	13.1	1.49	19400	1510	4380	279	57.8	455	54.6	2200	604
× 125	678	253	16	11.7	1.23	16000	1190	3500	273	44.1	349	52.5	1180	594
W610 × 195	622	327	24	15.4	1.91	24900	1680	5400	260	142	871	75.5	3970	554
× 155	611	324	19	12.7	1.51	19700	1290	4220	256	108	666	74.0	1950	545
× 125	612	229	20	11.9	1.22	15900	985	3220	249	39.3	343	49.7	1540	537
× 101	603	228	15	10.5	0.99	13000	764	2530	242	29.5	259	47.6	781	527
W530 × 182	551	315	24	15.2	1.78	23100	1240	4480	232	127	808	74.1	3740	492
× 150	543	312	20	12.7	1.47	19200	1010	3710	229	103	659	73.2	2160	487
× 109	539	211	19	11.6	1.06	13900	667	2480	219	29.5	280	46.1	1260	471
× 82	528	209	13	9.5	0.81	10500	479	1810	214	20.3	194	44.0	530	463
W460 × 144	472	283	22	13.6	1.41	18400	726	3080	199	83.6	591	67.4	2440	421
× 97	466	193	19	11.4	0.95	12300	445	1910	190	22.8	237	43.1	1130	408
× 82	460	191	16	9.9	0.80	10400	370	1610	189	18.6	195	42.3	691	404
× 61	450	189	11	8.1	0.60	7760	259	1150	183	12.2	129	39.7	289	395
W410 × 114	420	261	19	11.6	1.12	14600	462	2200	178	57.2	439	62.6	1490	376
× 74	413	180	16	9.7	0.73	9550	275	1330	170	15.6	173	40.4	637	364
× 60	407	178	13	7.7	0.58	7580	216	1060	169	12.0	135	39.8	328	363
× 39	399	140	9	6.4	0.38	4990	127	634	160	4.0	57.7	28.5	111	348
W360 × 314	399	401	40	24.9	3.07	39900	1100	5530	166	426	2120	103	18500	345
× 122	363	257	22	13.0	1.19	15500	365	2010	153	61.5	478	63.0	2100	322
× 79	354	205	17	9.4	0.78	10100	227	1280	150	24.2	236	48.9	814	317
× 64	347	203	14	7.7	0.63	8140	178	1030	148	18.8	186	48.1	438	312
× 45	352	171	10	6.9	0.44	5730	122	691	146	8.18	95.7	37.8	160	313
× 33	349	127	8	5.8	0.32	4170	82.7	474	141	2.91	45.8	26.4	85.9	305
W310 × 253	356	319	40	24.4	2.48	32200	682	3830	146	215	1350	81.7	14800	304
× 118	314	307	19	11.9	1.15	15000	275	1750	135	90.2	588	77.5	1600	282
× 79	306	254	15	8.8	0.77	10100	177	1160	132	39.9	314	62.9	657	277
× 60	303	203	13	7.5	0.59	7590	129	849	130	18.3	180	49.1	397	274
× 39	310	165	10	5.8	0.38	4940	85.1	549	131	7.27	88.1	38.4	126	279
× 21	303	101	6	5.1	0.21	2690	37.0	244	117	0.983	19.5	19.1	29.4	258
W250 × 115	269	259	22	13.5	1.12	14600	189	1410	114	64.1	495	66.3	2130	236
× 49	247	202	11	7.4	0.48	6250	70.6	572	106	15.1	150	49.2	241	223
× 33	258	146	9	6.1	0.32	4170	48.9	379	108	4.73	64.7	33.7	98.5	231
W200 × 59	210	205	14	9.1	0.58	7560	61.1	582	89.9	20.4	199	51.9	465	187
× 36	201	165	10	6.2	0.35	4580	34.4	342	86.7	7.64	92.6	40.8	146	181
× 27	207	133	8	5.8	0.26	3390	25.8	249	87.2	3.30	49.6	31.2	71.3	185
W150 × 30	157	153	9	6.6	0.29	3790	17.2	219	67.4	5.56	72.6	38.3	101	141
× 14	150	100	6	4.3	0.13	1730	6.87	91.5	63.0	0.92	18.4	23.0	17.0	133

87

Table 20.2 – Sawn Timber Section Table

Sawn Timber Sections
Dimensions and Section Properties

Size and Designation $b \times d$	Nominal Dimensions	Dead Load	Area	Strong Axis x-x			Weak Axis y-y			Torsion Constant
				I_x	S_x	r_x	I_y	S_y	r_y	J
mm	in.	kN/m	mm²	10^6 mm⁴	10^3 mm³	mm	10^6 mm⁴	10^3 mm³	mm	10^6 mm⁴
292 × 495	12 × 20	0.907	145000	2950	11900	143	1030	7030	84.3	2570
× 445	× 18	0.816	130000	2140	9640	129	923	6320	84.3	2190
× 394	× 16	0.722	115000	1490	7550	114	817	5600	84.3	1760
× 343	× 14	0.629	100000	982	5730	99.0	712	4870	84.3	1370
× 292	× 12	0.535	85300	606	4150	84.3	606	4150	84.3	1030
241 × 495	10 × 20	0.749	119000	2440	9840	143	577	4790	69.9	1600
× 445	× 18	0.673	107000	1770	7950	129	519	4310	69.6	1360
× 394	× 16	0.596	95000	1230	6240	114	460	3810	69.6	1130
× 343	× 14	0.519	82700	810	4730	99.0	400	3320	69.6	900
× 292	× 12	0.442	70400	500	3420	84.3	341	2830	69.6	671
× 241	× 10	0.365	58100	281	2330	69.6	281	2330	69.6	476
191 × 495	8 × 20	0.594	94600	1930	7800	143	287	3010	55.1	868
× 445	× 18	0.534	85000	1400	6300	129	258	2710	55.1	751
× 394	× 16	0.472	75300	974	4940	114	229	2400	55.1	636
× 343	× 14	0.411	65500	642	3750	99.0	199	2090	55.1	515
× 292	× 12	0.350	55800	396	2710	84.3	170	1780	55.1	403
× 241	× 10	0.289	46000	223	1850	69.6	140	1470	55.1	285
× 191	× 8	0.229	36500	111	1160	55.1	111	1160	55.1	188
140 × 445	6 × 18	0.391	62300	1030	4620	129	102	1450	40.4	325
× 394	× 16	0.346	55200	714	3620	114	90.1	1290	40.4	279
× 343	× 14	0.301	48000	471	2750	99.0	78.4	1120	40.4	232
× 292	× 12	0.257	40900	290	1990	84.3	66.8	954	40.4	186
× 241	× 10	0.212	33700	163	1360	69.6	55.1	787	40.4	139
× 191	× 8	0.168	26700	81.3	851	55.1	43.7	624	40.4	94.9
× 140	× 6	0.123	19600	32.0	457	40.4	32.0	457	40.4	54.2
89 × 387	4 × 16	0.216	34400	430	2220	112	22.7	511	25.7	77.5
× 337	× 14	0.188	30000	284	1680	97.3	19.8	445	25.7	65.9
× 286	× 12	0.160	25500	174	1210	82.6	16.8	378	25.7	53.8
× 235	× 10	0.131	20900	96.3	819	67.8	13.8	310	25.7	41.9
× 184	× 8	0.103	16400	46.2	502	53.1	10.8	243	25.7	30.1
× 140	× 6	0.078	12500	20.4	291	40.4	8.22	185	25.7	19.8
× 114	× 5	0.064	10200	11.0	193	32.9	6.70	151	25.7	13.8
× 89	× 4	0.050	7920	5.23	118	25.7	5.23	117	25.7	8.85
64 × 337	3 × 14	0.135	21600	204	1210	97.3	7.36	230	18.5	25.8
× 286	× 12	0.115	18300	125	872	82.6	6.25	195	18.5	21.4
× 235	× 10	0.094	15000	69.2	589	67.8	5.13	160	18.5	17.0
× 184	× 8	0.074	11800	33.2	361	53.1	4.02	126	18.5	12.5
× 140	× 6	0.056	8960	14.6	209	40.4	3.06	95.6	18.5	8.68
× 114	× 5	0.046	7300	7.90	139	32.9	2.49	77.8	18.5	6.41
× 89	× 4	0.036	5700	3.76	84.5	25.7	1.94	60.8	18.5	4.29
38 × 337	2 × 14	0.071	12800	121	719	97.3	1.54	81.1	11.0	5.72
× 286	× 12	0.060	10900	74.1	518	82.6	1.31	68.8	11.0	4.79
× 235	× 10	0.049	8930	41.1	350	67.8	1.07	56.6	11.0	3.87
× 184	× 8	0.038	6990	19.7	214	53.1	0.84	44.3	11.0	2.91
× 140	× 6	0.029	5320	8.69	124	40.4	0.64	33.7	11.0	2.11
× 114	× 5	0.024	4330	4.69	82.3	32.9	0.52	27.4	11.0	1.65
× 89	× 4	0.019	3380	2.23	50.2	25.7	0.41	21.4	11.0	1.19
× 64	× 3	0.013	2430	0.83	25.9	18.5	0.29	15.4	11.0	0.73
× 38	× 2	0.008	1440	0.17	9.15	11.0	0.17	9.15	11.0	0.29

Lecture 21 – Calculation of Flexural Stresses

Overview:

In this chapter, methods used to analyze the bending behaviour of more complex shapes are introduced. For these members, Navier's equation is still capable of determining the flexural stresses, but the location of the centroid and the second moment of area must be determined first.

Calculation of the Centroidal Axis

The centroidal axis is a key geometric property of a member when subjected to bending moments because other properties, like the second moment of area **I**, or the section modulus **S**, are calculated based on its location. For this reason, locating the centroidal axis is typically the first task done when approaching a bending problem. Recall from Lecture 20 that if the variable **y** is defined as the vertical distance between a point on the cross section and the neutral axis, then the following is true for members subjected to pure bending and no axial force:

$$0 = \int_A y\, dA \tag{21.1}$$

When performing calculations, we typically do not evaluate this integral analytically. A more convenient procedure is to instead break up the cross section into various simple shapes, and replace the integral with an algebraic sum:

$$0 = \int_A y\, dA = \sum_{i=1}^{n} y_i A_i \tag{21.2}$$

In Eq. (21.2), the cross section has been broken up into **n** discrete area components, A_i, and y_i is the vertical distance from the local centroid of the area component and the centroidal axis of the overall cross section. This is shown in Fig. 21.1.

Although Eq. (21.2) can be used to verify if the location of the centroidal axis has been correctly determined, it is less useful for actually determining where that axis is. The equation can be repurposed to solve for the location of the centroidal axis relative to the base of the cross section, $\bar{y}$, using the following coordinate transformation:

$$y_i = \bar{y} - y_{i,b} \tag{21.3}$$

In Eq. (21.3), $y_{i,b}$ is the vertical distance between the base of the cross section and the centroid of the area of interest. These various definitions of **y** are shown in Fig. 21.2. Substituting Eq. (21.3) into Eq. (21.2) results in the following:
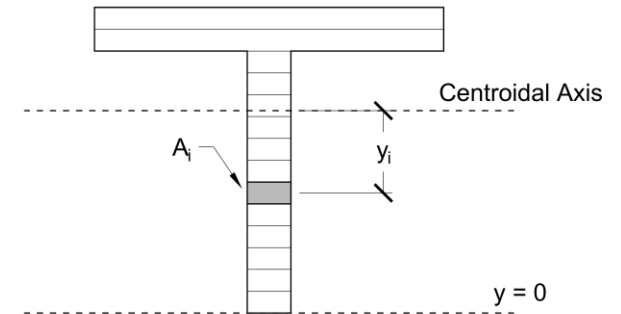
$$0 = \sum_{i=1}^{n} (\bar{y} - y_{i,b}) A_i \tag{21.4}$$

Fig. 21.1 – Definitions of A_i and y_i for evaluating the first moment of area using Eq. (21.2).

Note: If y_i is the distance from the centroid of the area component A_i to the centroidal axis of the whole cross section, then the summation term is an exact representation of the integral equation in Eq. (21.1).
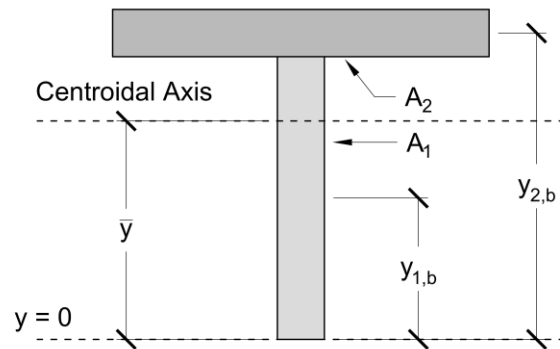
Fig. 21.2 – Definitions of terms used to calculate the location of the centroidal axis using Eq. (21.6)

Expanding the term in brackets and rearranging produces the following result:

$$\sum_{i=1}^{n} \bar{y} A_i = \sum_{i=1}^{n} y_{i,b} A_i \tag{21.5}$$

Finally, by recognizing that $\bar{y}$ is a constant, we can remove it from the summation term on the left-hand side of the equation, giving us a direct equation to obtain the location of the centroidal axis:

$$\bar{y} = \frac{\sum_{i=1}^{n} y_{i,b} A_i}{\sum_{i=1}^{n} A_i} = \frac{1}{A} \sum_{i=1}^{n} y_{i,b} A_i \tag{21.6}$$

In Eq. (21.6), **A** is the total area of the cross section. An example of using Eq. (21.6) to obtain the centroidal axis of the shape shown in Fig. 21.2 is shown below:

$$\bar{y} = \frac{y_{1,b} A_1 + y_{2,b} A_2}{A_1 + A_2} \tag{21.7}$$

Calculating I for Complex Shapes: Parallel Axis Theorem
The second moment of area, **I**, is defined by Eq. (21.8) shown below, where **y** is the vertical distance measured from the centroidal axis of the cross section, and **A** is the area of the cross section:

$$I = \int_A y^2 \, dA \tag{21.8}$$
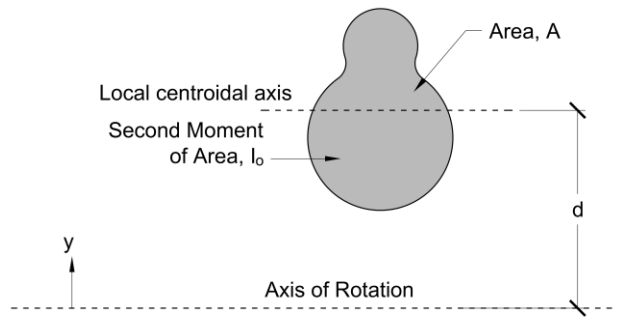
Fig. 21.3 – Schematic of a body rotating around an axis which is not its own local centroidal axis.

Table 21.1 – Equations for I for simple shapes

	Rectangle	Circle
Shape		
I_o	$I_o = \dfrac{bh^3}{12}$	$I_o = \dfrac{\pi d^4}{64}$

When calculating **I** for simple shapes, such as a rectangle or circle, Eq. (21.8) can be explicitly evaluated, resulting in the simple equations shown in Table 21.1. However, structural members often assume more complex shapes whose values of **I** cannot be easily determined by using Eq. (21.8) directly.

A convenient way of calculating **I** for more complex geometries is to first break up the cross section into **n** smaller components and determine their inertia about the global centroidal axis, **I_i**. The value of **I** of the cross section is then the sum of these individual components:

$$I = \sum_{i=1}^{n} I_i \tag{21.9}$$

When evaluating Eq. (21.9), the equations for **I_o** of rectangles and circles in Table 21.1 cannot be used directly because they are the second moments of area about the *local* centroidal axes of the shapes. This is different from **I_i,** which are the second moments of area about the *global* centroidal axis of the cross section. If the local centroid of the subcomponent area, **A_i** is a distance **d_i** from the axis of rotation like in the situation shown in Fig. 21.3, then Eq. (21.8) can be re-written as:
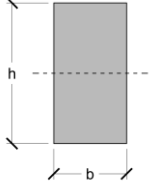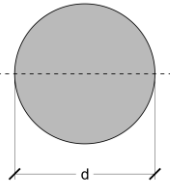
$$I_i = \int_{A_i} (y + d_i)^2 dA \tag{21.10}$$

Expanding the terms in brackets results in the following:

$$I_i = \int_{A_i} y^2 + 2d_i y + d_i^2 \, dA = \int_{A_i} y^2 dA + \int_{A_i} 2d_i y \, dA + \int_{A_i} d^2 dA \tag{21.11}$$

In Eq. (21.11), the first integral term is the second moment of area of the component if interest about its local centroidal axis, which we will define as **I_o,i**. For the second and third integrals, the distance **d_i** is not a function of the area and

can hence be moved outside of the integrals. The second term will then equal to zero, due to Eq. (21.1), which results in the following equation:

$$I_i = I_{o,1} + A_i d_i^2 \tag{21.12}$$

Eq. (21.12) is called the ***Parallel Axis Theorem*** and allows the second moment of area of a shape to be calculated about an axis of rotation which is parallel to its local centroidal axis. If the Parallel Axis Theorem is applied to each of the **n** subcomponents of the cross section, the second moment of area of the whole section can be calculated as:

$$I = \sum_{i=1}^{n} I_i = \sum_{i=1}^{n} (I_{o,i} + A_i d_i^2) \tag{21.13}$$

Fig. 21.4 shows an area as it rotates about an axis which is not aligned with its local centroidal axis. The total movement involves (1) its translation around the axis of rotation along a circular path, and (2) its rotation about its own centroid. Its total inertia is therefore the sum of its inertia against local rotation, $\mathbf{I_{o,i}}$, and its resistance to being translated around the global axis, which is represented by the $\mathbf{A_i d_i^2}$ term.
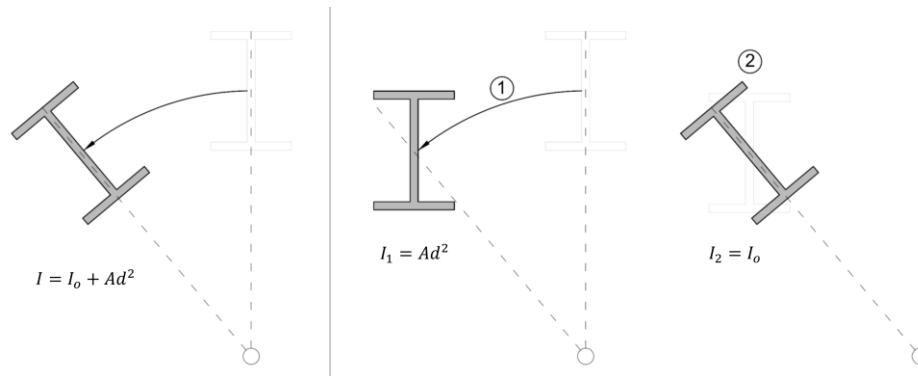
Fig. 21.4 – Illustration of the various displacements associated with the terms in the Parallel Axis Theorem.

Calculating I for Members with a Horizontal Axis of Symmetry

Many common structural shapes, like the hollow tube and I-beam shown in Fig. 21.5, have a horizontal axis of symmetry. This can be used to calculate **I** in a more convenient manner than using Eq. (21.13) by taking advantage of the fact that the $\mathbf{I_i}$ terms in Eq. (21.9) may be positive or negative. This is illustrated for the hollow tube in Fig. 21.5, where **I** is equal to second moment area of a solid rectangle defined by its outside dimensions minus the second moment of area of a solid rectangle defined by its inside dimensions. Likewise, for the I-beam, **I** can be easily found by subtracting the second moment of area of the inner rectangles from the second moment of area of a solid rectangle defined by the overall height and flange width.

Note: Directly adding and subtracting components is only possible if they share a common centroidal axis. If a component which is being added or subtracted has a different centroidal axis, the Parallel Axis Theorem must be applied.
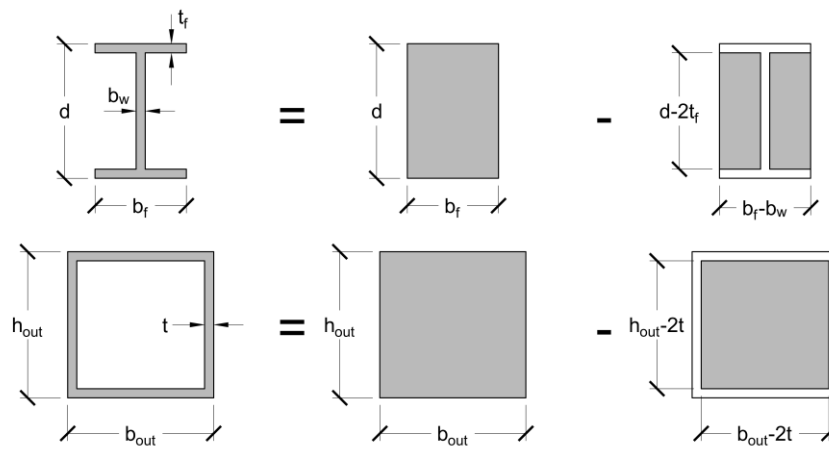
$$I = I_{out} - I_{in}$$

Shape	I_{out}	I_{in}
I beam	$I_{out} = \dfrac{b_f d^3}{12}$	$I_{in} = \dfrac{(b_f - b_w)(d - 2t_f)^3}{12}$
Hollow tube	$I_{out} = \dfrac{b_{out} h_{out}^3}{12}$	$I_{in} = \dfrac{(b_{out} - 2t)(h_{out} - 2t)^3}{12}$

Fig. 21.5 – Calculation of I for I beams and hollow sections by using horizontal symmetry

Summary

When approaching a problem involving flexure, the location of the centroidal axis, $\bar{y}$, and the second moment of area, I, must be determined in order to calculate other relevant parameters like the stresses, strains and curvature. The suggested procedure is as follows:

    i.   Break up the cross section in to simple shapes with area A_i and whose local centroids are a distance $y_{i,b}$ from the bottom of the member.

   ii.   Determine the location of the centroidal axis relative to the bottom of the member, $\bar{y}$, using Eq. (21.6), which is reproduced below:

$$\bar{y} = \frac{1}{A}\sum_{i=1}^{n} y_{i,b} A_i$$

  iii.   Calculate the distances between the local centroids of the component areas, and the centroidal axis of the global cross section, d_i.

   iv.   Using the Parallel Axis Theorem, calculate the second moment of area, **I**, using Eq. (21.13), which is reproduced below:

$$I = \sum_{i=1}^{n} I_{o,i} + A_i d_i^2$$

Lecture 22 – Shear Force Diagrams and Bending Moment Diagrams

Overview:
Having introduced the equations which allow the flexural stresses to be calculated if the bending moment carried by the section is known, the concept of stress resultants is presented in this chapter. The relevant methods for calculating the axial load, shear force, and bending moment diagrams for loaded members is presented.

Stress Resultants

Consider the simply supported beam shown in Fig. 22.1 which is carrying a variety of horizontal and vertical loads and transmitting them to the supports. As we saw earlier in the course where a wire transmitted a tension force by carrying internal stresses, this member will also be carrying substantial internal forces. These internal forces, which are called ***stress resultants***, can be found by drawing a free body diagram which cuts the member through a point of interest.

Note: The procedure of cutting through the member to determine the stress resultants is analogous to using the Method of Sections to determine the member forces in a truss.
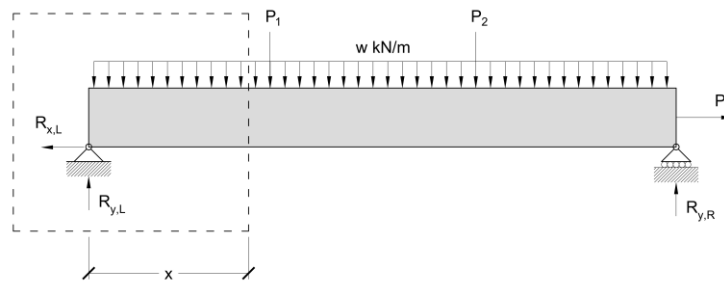
Fig. 22.1 – Simply supported beam subjected to arbitrary loading conditions:

Fig. 22.2 shows a free body diagram of a portion of the larger beam which has been cut at a distance **x** away from the left support. In order to satisfy horizontal, vertical, and rotational equilibrium, it must carry internal horizontal and vertical forces, as well as a moment at the location of the cut. The horizontal force which is parallel to its longitudinal axis is called the ***axial load***, **N**, the vertical force which is perpendicular to the longitudinal axis is called the ***shear force***, **V**, and the moment is called the ***bending moment***, **M**.

Note: The shear force is obtained by integrating the shear stresses carried by the member. Shear stresses will be discussed in more detail in Lecture 25.
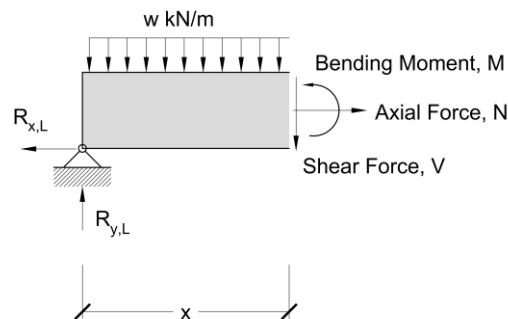

Fig. 22.2 – Section cut of member, revealing stress resultants N, V and M.

Applying the equilibrium equations to the free body diagrams allows these stress resultants to be directly calculated in terms of the applied loads and the reaction forces. If the free body diagram in Fig. 22.2 is valid from x = 0 until just before the first downwards point load from the left, then the stress resultants can be calculated to be:

$$\sum F_x = 0 \rightarrow N = R_{x,L} \tag{22.1}$$

$$\sum F_y = 0 \rightarrow V = R_{y,L} - wx \tag{22.2}$$

$$\sum M_o = 0 \rightarrow M = R_{y,L}x - (wx)\left(\frac{1}{2}x\right) \tag{22.3}$$

As seen from Eqs. (22.1) to (22.3), the stress resultants generally change along the length of the member, based on the loading. In structural engineering, we typically use diagrams to show the change in the axial load, shear force and bending moment along the member instead of using mathematical representations like in the equations above.

As noted in earlier lectures, the stresses carried by the material are related to the stress resultants; knowing how the values of **N**, **V** and **M** vary along the entire member is necessary to determine when it will fail or to design it to safely carry the applied loads.

Shear Force Diagrams
The shear force diagram represents the net vertical force which is carried by the member at a given location and can be obtained once the reaction forces are known. The shear force is related to the vertical loads applied to the structure, **w(x)** by the following relationship:

$$w(x) = \frac{d}{dx}V(x) \tag{22.4}$$

Note: The sign convention for Eq. (22.4) and (22.5) is that load which act upwards will cause the shear force to become more positive, and loads which act downwards will cause the shear force to become more negative.

According to Eq. (22.4), the change in the shear force at a given location is equal to the loading which is applied at to the member to that section. From this we can conclude that a uniformly distributed load would cause the shear force to vary linearly over the length, and a concentrated point load would cause a sudden change in the shear force diagram. Using the Fundamental Theorem of Calculus, the change in the shear force between two points along the member which are subjected to the loading **w(x)** can be calculated as:

$$\Delta V_{AB} = V_B - V_A = \int_A^B w(x)dx \tag{22.5}$$

Eq. (22.5) provides a means to calculate the shear force at any point along the member based on the given loading. Taking point A as the left side of the member where x = 0 and choosing point B as an arbitrary location which is x away from point A, then Eq. (22.5) can be summarized using the following heuristic for finding the shear force at any location along the member:
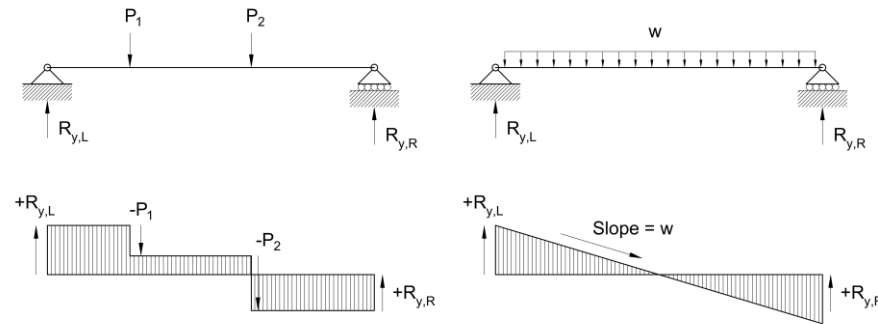
Fig. 22.3 – Examples of obtaining the shear force diagram using the reaction forces and applied loads

Note: this heuristic can also be applied by using the right side of the member as the starting point instead of the left side.

The shear force in the member at a given location is the cumulative sum of the vertical forces applied to the member from the left end of the member to the location of interest.

Fig. 22.3 illustrates the application of Eq. (22.4) and (22.5) to draw the shear force diagrams for two simple structures. As a consequence of Eq. (22.4), the shear force has sudden jumps at locations where there is a concentrated reaction force or load, as seen in the left example. In the right example, the beam is carrying a uniformly distributed load, which results in the shear force decreasing linearly along the length of the beam. For both examples, the shear force diagram returns to zero at the right-hand side, indicating that the sum of the vertical forces over the entire member equal to zero and the member is in vertical equilibrium.

Bending Moment Diagrams:
The bending moment diagram is related to the shear force diagram by the following relationships:

Note: According to this definition, regions of high shear correspond to steep portions on the bending moment diagram. Regions of low shear correspond to comparatively flat portions on the bending moment diagram.

$$V(x) = \frac{d}{dx}M(x) \qquad (22.6)$$

Eq. (22.4) states that the change in moment at a given section is equal to the shear force carried by the member at that location. In regions where there are large shear forces, the moment will change rapidly. Because the shear force is the derivative of the bending moment, a constant shear of $V = 0$ will cause the moment diagram to be constant, a constant nonzero shear force will cause the bending moment diagram to vary linearly, and a linearly varying shear force will cause the bending moments to vary quadratically. Using the Fundamental Theorem of Calculus, the change in moment, ΔM, between two points can then be related to the shear force, $V(x)$, according to the following equation:

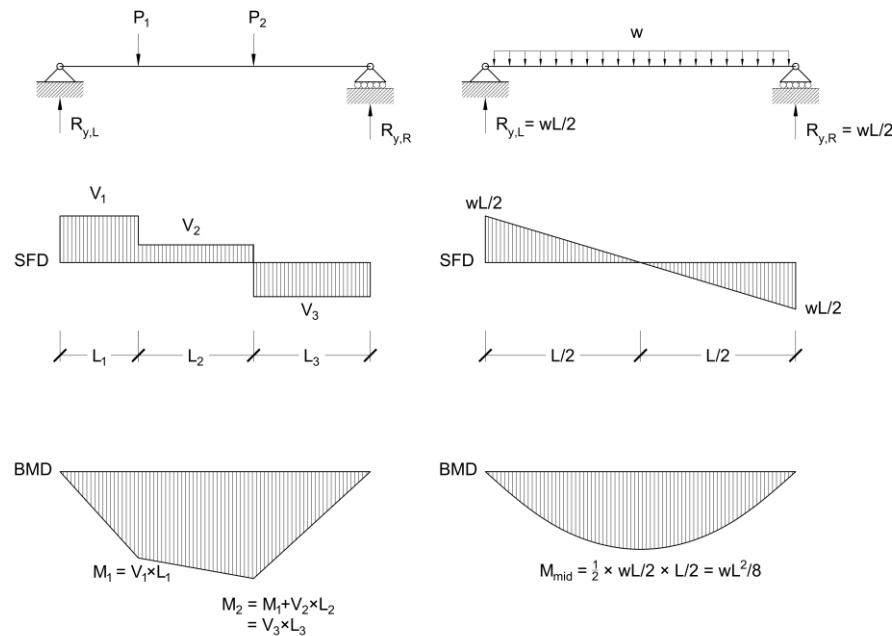$$\Delta M_{AB} = M_B - M_A = \int_A^B V(x)dx \qquad (22.6)$$

Fig. 22.4 – Examples of obtaining bending moment diagram using the shear force diagram

Eq. (22.6) states that the change in moment between two points, A and B, is equal to the area underneath the shear force diagram between these locations. Therefore, if the moment is known at the ends of the member, then the moment at any location can be computed using Eq. (22.6) once the shear force diagram has been drawn.

Fig. 22.4 shows the same structures analyzed in Fig. 22.3 and the corresponding shear force diagrams and bending moment diagrams. For the structure on the left, the bending moment diagram is a series of connected lines because the shear force is constant between the applied loads. The change in moment between points is also equal to the area under the shear force diagram between them. For the uniformly distributed beam on the right, the bending moment diagram follows the shape of a parabola because the shear for diagram is linearly varying. Near the supports where the shear force is high, the slope of the bending moment diagram is also high, and at the midspan, where the shear force is equal to zero, the slope of the moment diagram is equal to zero, indicating that it has reached its maximum value. For both structures, the bending moment diagram begins at zero on the left-hand side and returns to zero at the right-hand side, indicating that the sum of moments over the member equals to zero, and the member is in rotational equilibrium.

Note: This condition where the moment equals zero over a support is only true if the ends of the structure are supported by a pin or roller. In general, the moment will not equal to zero over a pin or roller support if the support is located at an intermediate location.

Note: The bending moment at the location of an internal hinge is equal to zero because the hinge will freely rotate if it tries to carry a moment.

Sign convention

Determining the sign of the shear force diagram and the bending moment diagram can be non-intuitive at first. Fig. 22.5 shows the sign convention for shear force; a general heuristic is that upwards-acting forces induce positive shear forces into the member, while downwards-acting forces induce negative shear forces into the member.
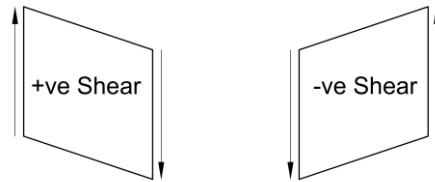

Fig. 22.5 – Sign convention for shear force

The sign convention for bending moments is shown in Fig. 22.6. Positive moment (which is unintuitively drawn on the bending moment diagram below the axis) corresponds to regions where the bottom of the member is in tension, and negative moment (drawn above the axis) corresponds to regions where the top of the member is in tension. When determining the bending moment diagram from the shear force diagram, a useful heuristic is to note that positive shear results in positive moment (which goes downwards on the bending moment diagram), whereas negative shear results in negative moment (which goes upwards on the bending moment diagram).
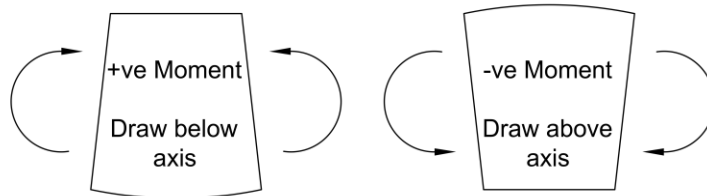

Fig. 22.6 – Sign convention for bending moments

Lecture 23 – Deflection of Beams: Moment Area Theorems

Overview:
Like trusses, obtaining the deformed geometry of a member which is bending can require very complex calculations. In this chapter, the Moment Area Theorems, which permit the deflection of beams to be obtained in a relatively straightforward manner, are presented.

Curvature Diagram
When working on a problem involving beams, the reaction forces, shear force diagram, and bending moment diagram are typically obtained first. Using these diagrams, the flexural stresses can then be calculated once the relevant section properties, like the location of the centroidal axis and the second moment of area, are known. All of this information is necessary to begin calculating qualities relating the deformed shape of the member, like its displacement and slope at key points of interest.

The curvature of a member, ϕ, is related to the bending moment, **M**, and the flexural stiffness, **EI**, at any given point by the following equation:

$$\phi = \frac{M}{EI} \tag{23.1}$$

Fig. 23.1 – Summary of Moment Area Theorem #1

The curvature at every point can be calculated using the bending moment diagram and the flexural stiffness, producing a corresponding *curvature diagram*.

Moment Area Theorem #1
Recall that the curvature of a member is a measure of how bent it is, and is defined as the change in slope, θ, per unit length along the member:

$$\phi = \frac{d\theta}{dx} \tag{23.2}$$

Using the Fundamental Theorem of Calculus, the change in slope between two points, $\Delta\theta_{AB}$, is therefore defined as the integral of the curvature between points A and B. This is mathematically defined in Eq. (23.3) below and represents the area underneath the curvature diagram between the two points.

$$\Delta\theta_{AB} = \theta_B - \theta_A = \int_A^B \phi(x)dx \tag{23.3}$$

Eq. (23.3) is the first Moment Area Theorem, which states:

> *The change in slope between any two sections of a deflected beam is equal to the area under the curvature diagram between those two sections.*

The first Moment Area Theorem allows us to obtain the slope at any location using the curvature diagram if the slope is already known at some point along the member. This is illustrated in Fig. 23.1.
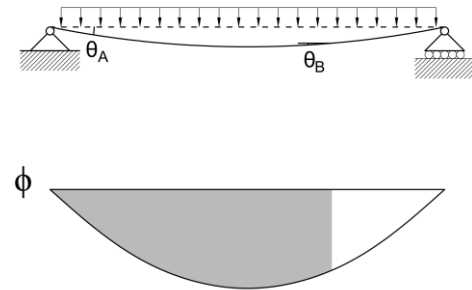
Moment Area Theorem #2

Careful integration of the curvature diagram can also be useful for calculating the displaced shape of a member. Consider the curved member shown in Fig. 23.2 which has two points, D and T, defined. Points D and T are located at arbitrary distance x_D and x_T from the original respectively in the horizontal direction.

Note: Displacements can be obtained by drawing a slope diagram using Eq. (23.3) and then integrating it to find a complete profile of the displaced shape of the member. However, this process is difficult to do analytically except for very simple geometries and loading conditions.
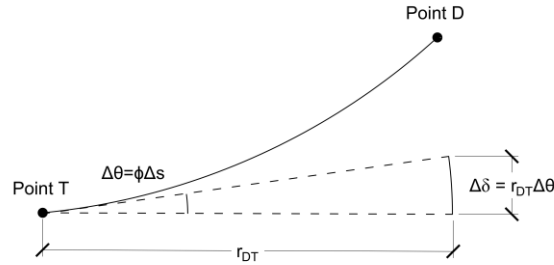
Fig. 23.2 – Curved member used to derive Moment Area Theorem #2

Consider a small length of the beam, **ds**, which is located at point T. The curvature at this location is equal to $\phi(x_T)$; if **ds** is very short distance, then the change in slope of the beam between $x = x_T$ and $x = x_T$ - ds is approximately equal to the following:

$$\Delta\theta(x = x_T) \cong \phi(x_T)\Delta s \tag{12.4}$$

Fig. 23.2 shows this change in angle at point T. If we define the distance $\mathbf{r_{DT}}$ as the distance between point T and a location directly below point D which is measured along the tangent at point T, then the arc length swept by this tangent, **dδ**, over the angle **dθ** is equal to:

$$\Delta\delta = r_{DT}\Delta\theta(x = x_T) \cong r_{DT}\phi(x_T)\Delta s \tag{12.5}$$

In structural engineering, members tend to have relatively small curvatures and associated displacements. This allows us to approximate the distance along the member, **ds**, as a distance in the horizontal direction, **dx**. Furthermore, the distance along the tangent, $\mathbf{r_{DT}}$, is now the horizontal distance between points D and T, $\mathbf{x_{DT}}$, and **dδ** becomes a vertical distance **dy**. These approximations allow Eq. (12.5) to be rewritten as:

$$\Delta y_{DT} = x_{DT}\phi(x_{DT})\Delta x \tag{12.6}$$

Eq. (12.6) represents the vertical distance between a tangent drawn at point T towards point D as the tangent traverses over a small angle **dθ**. The total vertical distance between a tangent drawn at point T and point D for the curved beam, $\mathbf{\delta_{DT}}$, can be obtained if we repeat the process for the entire length of the beam between points D and T, resulting in the following integral in the limit where $\Delta\mathbf{x}$ goes to zero:

$$\delta_{DT} = \lim_{\Delta x \to 0} \sum x\phi(x)\Delta x = \int_D^T x\phi(x)dx \tag{12.7}$$

The integral term in Eq. (12.7) represents the first moment of the area underneath the curvature diagram between points D and T taken about point D. This quantity can be calculated by obtaining the area under the curvature diagram between points D and T, then multiplying this area by the distance between its centroid and point D, $.\bar{x}_{DT}$ .This is mathematically represented using the following equation:

$$\delta_{DT} = \int_D^T x\phi(x)dx = \bar{x}_{DT} \int_D^T \phi(x)dx \tag{12.8}$$

Eq. (12.8) is the second Moment Area Theorem, which is illustrated in Fig. 23.3 and states:

> ***For any two points, called D and T, along the length of a deflected beam, the deviation of point D from the tangent drawn at point T equals the area under the curvature diagram between points D and T, times the distance from the centroid of the diagram to point D (i.e. the first moment of area about point D).***

Although the second Moment Area Theorem does not allow us to directly calculate the displacements of a beam, it is possible to express the desired displacement in terms of tangential deviations, **δ$_{DT}$**, which can be calculated using Eq. (12.8). When using the theorem, points D and T must be correctly indicated in order to obtain the desired value:

- D is the location where the tangential deviation is being <u>measured</u>
- T is the location where the tangent is <u>drawn</u>

Based on these definitions, the curvature diagram is integrated between points D and T, and that area is multiplied by the distance between its centroid and point D, the location where the deviation is being measured.

Areas and Centroids of Common Shapes
When using the Moment Area Theorems, the areas and centroids of many different curvature distributions will need to be obtained. Table 23.1 provides a series of simple expressions for these areas and centroids of many common shapes, and is a convenient alternative to analytically integrating the curvature diagram. For distributions which are not shown in the table but can be broken up into **n** simpler subcomponents, the two theorems can be applied by summing of the contributions of the smaller parts to $\Delta\boldsymbol{\theta}$ or $\boldsymbol{\delta}$. This modifies Eqs. (23.3) and (23.8) to be the following:

$$\Delta\theta_{AB} = \int_A^B \phi(x)dx = \sum_{i=1}^n \left[\int \phi(x)dx\right]_i \tag{23.9}$$

$$\delta_{DT} = \int_D^T x\phi(x)dx = \bar{x}_{DT} \int_D^T \phi(x)dx = \sum_{i=1}^n \left[\bar{x}\int \phi(x)dx\right]_i \tag{23.10}$$
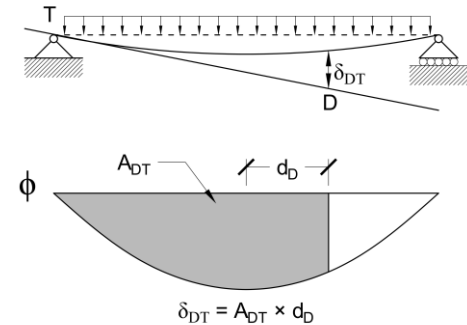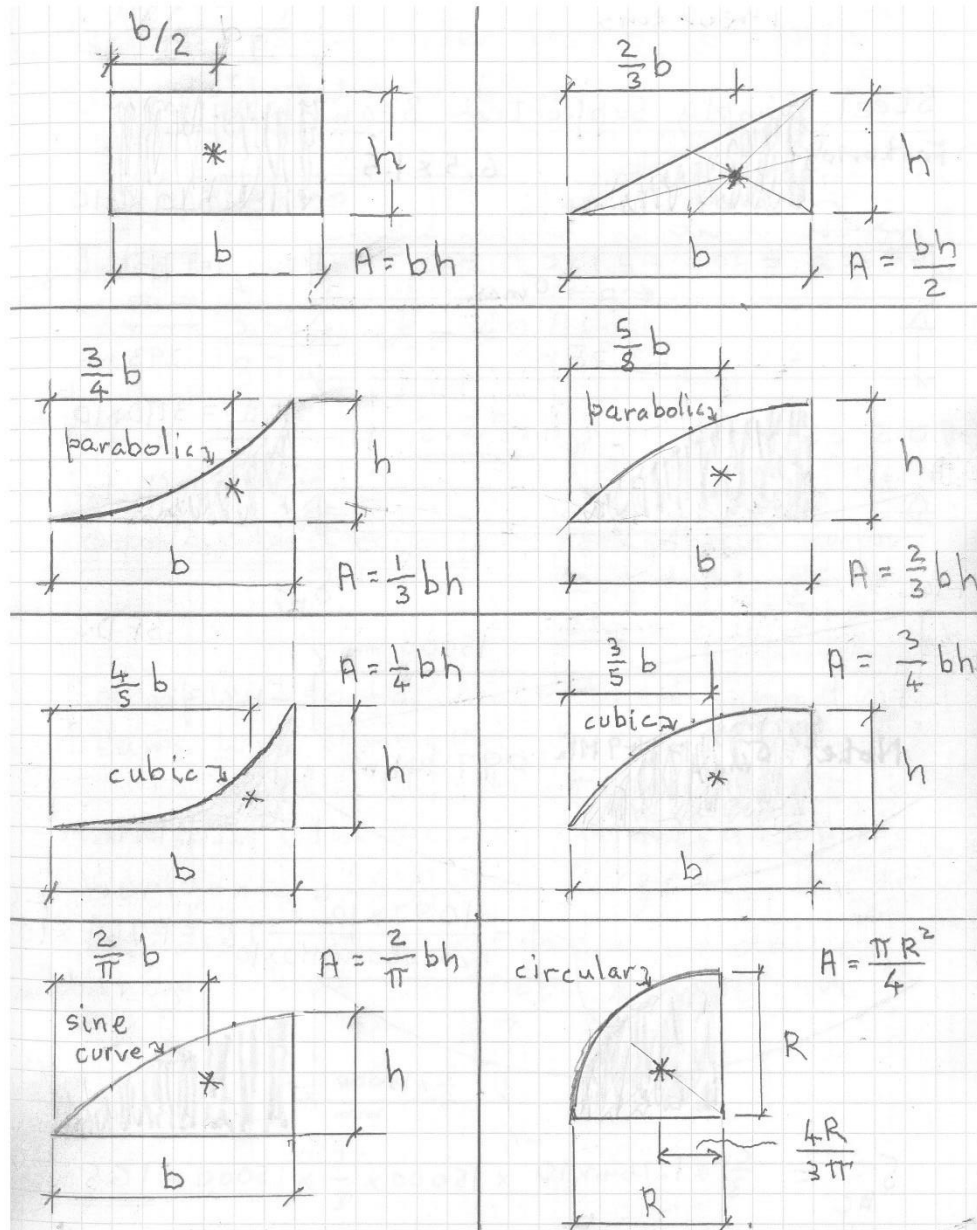

Fig. 23.3 – Summary of Moment Area Theorem #2

Table 23.1 – Areas and centroids of common shapes

Lecture 24 – Using Moment Area Theorems

Overview:

This chapter demonstrates how to use the Moment Area Theorems presented in Lecture 23 to solve for displacements and rotations in simple structures under common loading situations.

General Procedure:

In addition to being designed to be strong, structures must also have adequate stiffness, so they do not experience unreasonable deformations when carrying loads. Two measures of how deformed a member is are its slope, θ, and how much it has displaced from its original position, Δ.

The two Moment Area Theorems introduced in Lecture 23 provide the means to obtain quantities related to the displaced shape of a loaded member. The first Moment Area Theorem (MAT1) allows us to calculate the change in angle between two locations, $\Delta\theta_{AB}$, by finding the area under the curvature diagram between these two points; this is mathematically represented in Eq. (24.1):

$$\Delta\theta_{AB} = \theta_B - \theta_A = \int_A^B \phi(x)dx \tag{24.1}$$

The second Moment Area Theorem (MAT2) allows us to calculate the vertical distance between a point on the displaced member, point D, and a tangent which is drawn from another point on the displaced member, point T. This distance, the tangential deviation of point D from a tangent drawn at point T, is equal to the area of the curvature diagram between points D and T multiplied by the distance between its centroid and point D:

$$\delta_{DT} = \int_D^T x\phi(x)dx \tag{24.2}$$

Although the two Moment Area Theorems allow displacement-related quantities about the structure to be obtained, they do not allow us to directly calculate the slope or deflection of the deformed member at a specific point of interest. Instead, they must be used together with other information about the structure – such as how it is loaded and how it is supported – to obtain the displacements and slopes.

A general procedure for calculating the slopes and displacements of a loading member is the following:

i.   Calculate the reaction forces and draw the shear force, bending moment, and curvature diagrams
ii.   Sketch out an approximate shape of the deformed structure
iii. Identify any locations where the deflection and slope of the member are known by considering the supports and loading conditions. Locations where the tangent is horizontal are particularly helpful.
iv.   Calculate the slope at a location of interest by using a known angle and Moment Area Theorem no. 1.
v.   Express the desired displacement in terms of tangential deviations which can be calculated using Moment Area Theorem no. 2 and solve.

This general procedure will be illustrated using three common scenarios.

Scenario 1 – Known Horizontal Tangent due to a Support Condition

Consider the cantilever structure shown in Fig. 24.1 which is carrying a point load which is located at its tip. The fixed end restrains the member from rotating, and hence the slope of the member at the support remains flat even when the member curves under the load. Therefore, a tangent which touches this point will be horizontal, as shown in the second drawing in Fig. 24.1 Since the fixed end also prevents the member from translating at this point, the tangent effectively acts along the undeformed length of the member.

1 - Undeformed Geometry and Loads   3 - Displaced Shape

2 - Curvature Diagram   4 - Calculation of tangential deviation
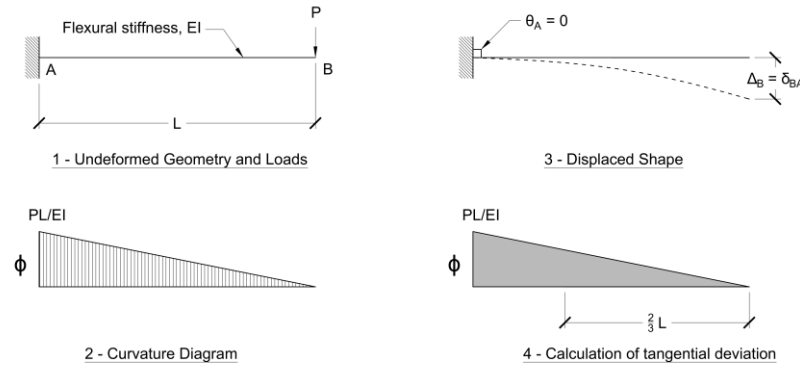
Fig. 24.1 – Undeformed (left) and deformed (right) geometry of a loaded cantilever

Calculating the slope at any point along the member can be done using MAT1 using the knowledge that $\theta_A = 0$ due to the fixed end. For example, the slope of the member at the tip, θ_B, is equal to the area under the full curvature diagram as shown below:

$$\Delta\theta_{AB} = \theta_B - 0 \rightarrow \theta_B = \int_{x=0}^{x=L} \phi(x)dx \qquad (24.3)$$

Evaluating this integral results in the following expression for the slope at the tip:

$$\theta_B = \frac{1}{2} \times L \times \frac{PL}{EI} = \frac{PL^2}{2EI} \qquad (24.4)$$

The horizontal tangent at the fixed end is also useful for evaluating the vertical displacement of the cantilever at any point because the deviation of the displaced member from that horizontal tangent is simply equal to the displacement. For example, the displacement of the tip, Δ_B, can be written as the tangential deviation of point B from a tangent drawn at the fixed end:

$$\Delta_B = \delta_{BA} \qquad (24.5)$$

Evaluating the tangential deviation results in the following expression for Δ_B:

$$\Delta_B = \left(\frac{1}{2} \times L \times \frac{PL}{EI}\right) \times \left(\frac{2}{3} \times L\right) = \frac{PL^3}{3EI} \qquad (24.6)$$

Scenario 2 – Known Horizontal Tangent due to Symmetrical Loading Conditions

When a structure is subjected to symmetrical loading conditions, this sometimes results in the location of a horizontal tangent being known. Consider the symmetrical beam shown in Fig. 24.2 which supports a point load at its midspan. It can be deduced that the maximum displacement occurs at the midspan, which implies that a tangent which touches this point is horizontal. The deformed shape of the beam and this horizontal tangent are shown in the Fig. 24.2 as well.
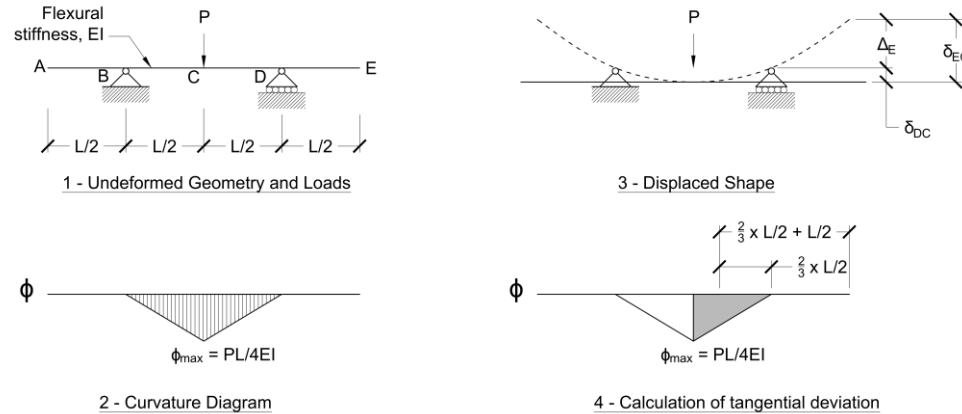
Fig. 24.2 - Undeformed (left) and deformed (right) geometry of a symmetrically loaded beam

As with the previous scenario, the slope of the member at any location along its length can be determined by using the slope at the midspan, $\theta_C = 0$, as a reference. For example, the slope at the right support, $\boldsymbol{\theta_D}$, is equal to the area underneath the curvature diagram between points C and D:

$$\Delta\theta_{CD} = \theta_D - 0 \rightarrow \theta_D = \int_C^D \phi(x)dx \tag{24.7}$$

Evaluating the area underneath the curvature diagram between points C and D results in the following expression for $\boldsymbol{\theta_C}$:

$$\theta_D = \frac{1}{2} \times \frac{L}{2} \times \frac{PL}{4EI} = \frac{PL^2}{16EI} \tag{24.8}$$

The horizontal tangent at the midspan is also useful for determining the vertical displacements at other points along the member. Suppose the upwards displacement of the tip, $\boldsymbol{\Delta_E}$, is desired. As shown in Fig. 24.2, this displacement can be calculated by taking the tangential deviation of point E from the tangent at C, and subtracting the deviation of the support, point D, from the same tangent:

$$\Delta_E = \delta_{EC} - \delta_{DC} \tag{24.9}$$

δ_{EC} and δ_{DC} are calculated by obtaining the area beneath the curvature diagram between points EC and DC respectively and multiplying this area by the distance from the centroid of the area to the location where the deviation is being calculated. In the case of δ_{EC}, this results in the following:

$$\delta_{EC} = \left(\frac{1}{2} \times \frac{L}{2} \times \frac{PL}{4EI}\right) \times \left(\frac{2}{3} \times \frac{L}{2} + \frac{L}{2}\right) = \frac{5PL^3}{96EI} \tag{24.10}$$

δ_{DC} is calculated as:

$$\delta_{DC} = \left(\frac{1}{2} \times \frac{L}{2} \times \frac{PL}{4EI}\right) \times \left(\frac{2}{3} \times \frac{L}{2}\right) = \frac{PL^3}{48EI} \tag{24.11}$$

Substituting the results of Eqs. (24.10) and (24.11) into Eq. (24.9) results in Δ_E being equal to:

$$\Delta_E = \frac{5PL^3}{96EI} - \frac{PL^3}{48EI} = \frac{PL^3}{32EI} \tag{24.12}$$

Scenario 3 – No Known Horizontal Tangents
In many instances, structures will be subjected to nonsymmetric loading, which means that the location of the maximum displacement (and therefore the horizontal tangent) cannot be determined without detailed calculations. An example of this is the simply supported beam carrying a point load located L/3 away from its right support in Fig. 24.3.

Note: The maximum displacement does not occur right underneath the applied load. It occurs where the slope of the beam is equal to zero (which cannot usually be determined from inspection).
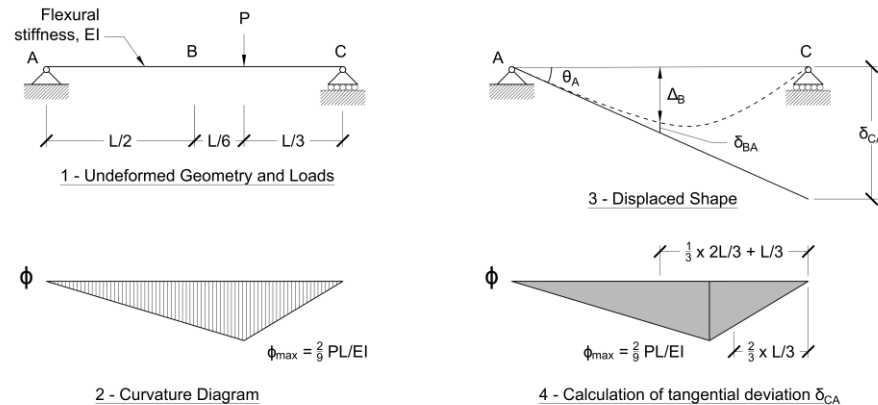

Fig. 24.3 - Undeformed (left) and deformed (right) geometry of an asymmetrically loaded beam

Despite the lack of a known angle or flat tangent, the displacements and slopes can still be obtained by determining the deviation of one support from a tangent to the other support, like in the right drawing in Fig. 24.3. If we assume that the beam is experiencing small deformations, then the slope at support A is approximately equal to:

$$\theta_A \cong \frac{\delta_{CA}}{L} \tag{24.13}$$

The tangential deviation δ_{CA} can be calculated by dividing the curvature diagram into two triangles, resulting in the following expression:

$$\delta_{CA} = A_1 d_1 + A_2 d_2 = \left(\frac{1}{2} \times \frac{2}{3}L \times \frac{2PL}{9EI}\right) \times \left(\frac{L}{3} + \frac{1}{3} \times \frac{2}{3}L\right) + \left(\frac{1}{2} \times \frac{L}{3} \times \frac{2PL}{9EI}\right) \times \left(\frac{2}{3} \times \frac{L}{3}\right) = \frac{4PL^3}{81EI} \tag{24.14}$$

Therefore, θ_A can be calculated using Eq. (24.13) and used as a reference to find the slope anywhere else along the member:

$$\theta_A = \frac{4PL^2}{81EI} \tag{24.15}$$

Suppose the displacement at the midspan, Δ_B, was of interest. This displacement can be obtained by drawing a similar triangle which relates the triangle outlined by the tangent and δ_{CA} to another triangle outlined by the tangent and the vertical distance between the tangent and the original position of the beam at the midspan. Using similar triangles results in the following equation:

$$\theta_A = \frac{\delta_{CA}}{L} = \frac{\Delta_B + \delta_{BA}}{0.5L} \tag{24.16}$$

Therefore, if the deviation of the midspan from a tangent drawn at support A is known, then Δ_B can be calculated by using Eq. (24.16). This deviation, δ_{BA}, can be found by using MAT2, resulting in:

Note: the 3/4 factor in Eq. (24.17) is used to obtain the curvature at the midspan by scaling the curvature underneath the point load.

$$\delta_{BA} = \left(\frac{1}{2} \times \frac{L}{2} \times \left(\frac{3}{4}\right) \times \frac{2PL}{9EI}\right) \times \left(\frac{1}{3} \times \frac{L}{2}\right) = \frac{PL^3}{72EI} \tag{24.17}$$

Re-arranging Eq. (24.16) substituting our results from Eqs. (24.14) and (24.17) allows Δ_B to be obtained:

$$\Delta_B = \frac{1}{2} \times \delta_{CA} - \delta_{BA} = \frac{7PL^3}{648EI} \tag{24.18}$$

Lecture 25 – Shear Stresses in Beams

Overview:

High shear forces carried by short members can lead to shear failures. In this chapter, the concept of shear stresses is introduced and Jourawski's equation for obtaining these shear stresses is derived.

Shear Stresses:

Shear stresses are the stresses which occur in structures which are carrying a shear force which is perpendicular to their longitudinal axis. Like axial stresses, σ, the shear stress, τ, is equal to the force applied parallel to a surface, V, divided by the area over which it acts, A:

$$\tau = \frac{V}{A} \tag{25.1}$$

Fig. 25.2 shows a small square element cut from a larger beam which is carrying vertical shear stresses on its left and right faces. Although the stresses on the two sides satisfy vertical equilibrium, they produce a couple which tends to cause the element to rotate. Therefore, ***complementary shear stresses*** exist on the top and bottom faces to satisfy rotational equilibrium. These shear stresses can be resolved into tensile and compressive stresses which act diagonally.

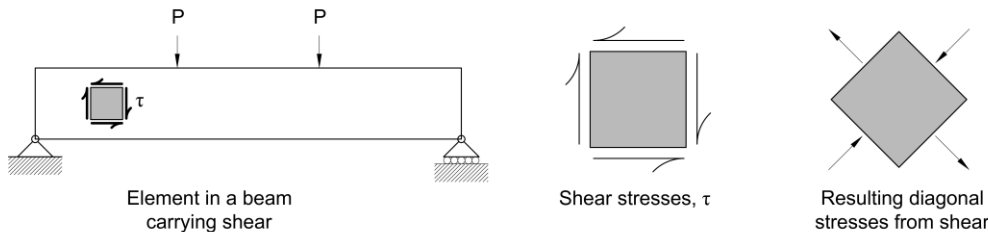Fig. 25.1 – Summary of Jourawski's equation for shear stresses in beams

Fig. 25.2 – Shear stresses in beams (left), elements in pure shear (centre), resulting diagonal stresses (right)

Axial stresses, which are associated with axial strains, ε, tend to cause materials to change volume by causing an expansion or contraction of the material. This volume change does not however affect the overall shape of the material. Shear stresses, which are associated with shear strains, γ, tend to cause materials to change shape while maintaining their volume. This is illustrated in Fig. 25.3.
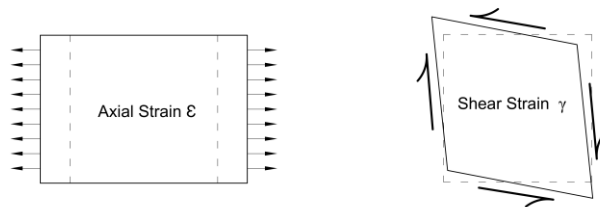

Fig. 25.3 – Comparison of axial deformations (left) and shear deformations (right)
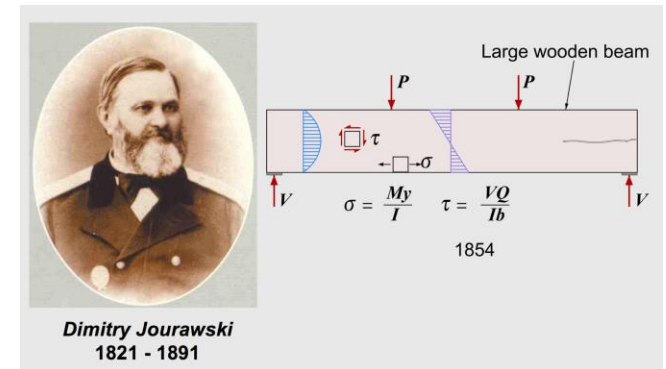
Shear stresses produce failures which are very different than the failures associated with axial loads and bending moments, which are instead associated with axial stresses. Some of examples of how shear causes structural failures are illustrated in Fig. 25.4. The first mode of failure, which can occur in wooden members, is a failure caused by the sliding of adjacent elements which carry shear stresses. The second mode of failure is caused by the diagonal tensile stresses associated with shear, which can cause failures in brittle materials like concrete. A third mode of failure which is not shown is caused by the diagonal compressive stresses associated with shear, which may lead to diagonal buckling of thin members.
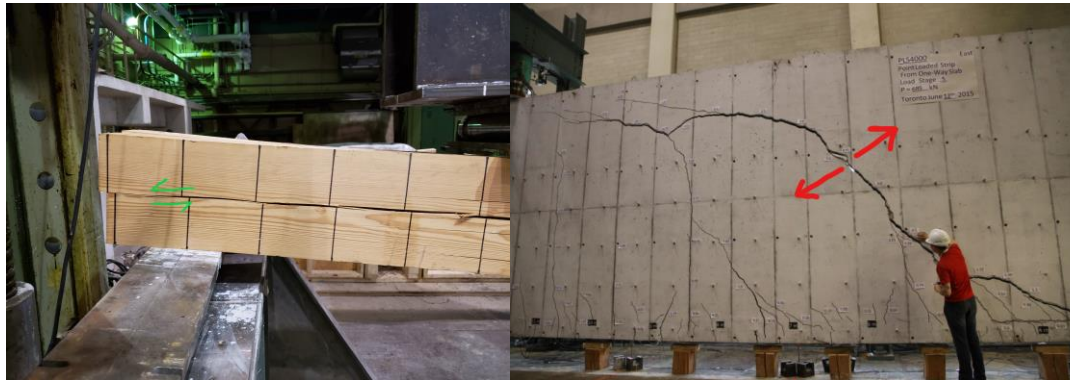

Fig. 25.3 – Failures associated with shear stresses – sliding between the fibres of a wooden beam (left) and diagonal cracking in a concrete beam (right)

Although Eq. (25.1) is a simple definition of the shear stress, calculating these stresses in beams which carry shear forces is more complicated because these shear stresses are not constant over the cross section. Instead, Jourawski's equation, shown below in Eq. (25.2), must be used to find them:

$$\tau = \frac{VQ}{Ib} \qquad (25.2)$$

Derivation of Jourawski's equation
Consider a beam which is carrying loads that are perpendicular to its longitudinal axis. Recall that the relationship between the bending moment and the shear force is:

$$V = \frac{dM}{dx} \qquad (25.3)$$

Therefore, in regions where there are shear forces, the moment will be changing along the length of the beam. This changing moment means that the flexural stresses will also be varying along the member as well.

Fig. 25.5 shows a portion of a beam which has a length of $\Delta\mathbf{x}$ which has been sliced out of a region of a beam which is carrying shear. For simplicity, the cross-section of the beam is a rectangle with width **b** and second moment of area **I**. On the left side of the beam, the moment will be equal to **M**, while on the right side of the beam, the moment carried by the section will be slightly larger, $\mathbf{M} + \Delta\mathbf{M}$.
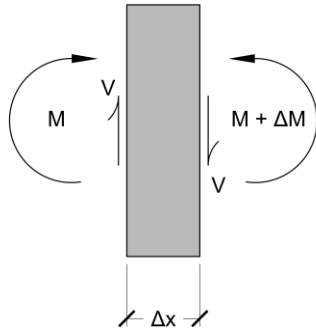
Fig. 25.5 – Slice of a beam carrying bending moments and shear forces
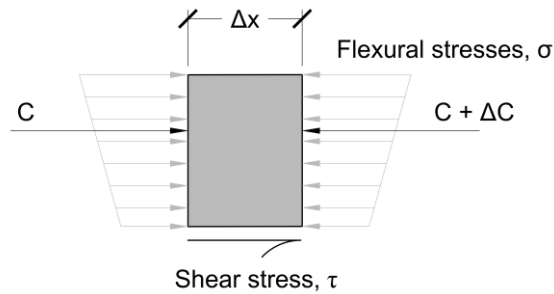
Fig. 25.6 – Free body diagram showing how shear stresses provide horizontal equilibrium

We can obtain an expression for the shear stress at a particular depth of this beam by drawing a free body diagram which cuts through this body to an arbitrary depth of interest, like the one shown in Fig. 25.6. The flexural stresses applied to this body cause it to be in compression, and because the moment is higher on the right side, the body will have a tendency to be pushed to the left. The net force which pushes the body to the left, **ΔC**, is caused by the increment in moment, **ΔM**, and is equal to:

$$\Delta C = \int_{y=A}^{y=y_{top}} \sigma(y)dy = \int_{y=A}^{y=y_{top}} \frac{\Delta My}{I}dy \tag{25.4}$$

Eq. (25.4) can be simplified by removing the constants **ΔM** and **I** from the integral, and representing the integral, which is a first moment of area about the centroidal axis of the member, as the quantity **Q**:

$$\Delta C = \frac{\Delta M}{I}\int_{y=A}^{y=y_{top}} ydy = \frac{\Delta M}{I}Q \tag{25.5}$$

In order to satisfy horizontal equilibrium, there must be a companion force which resists **ΔC**. This resisting force is provided by the shear stresses acting on the underside of the body, which produce an equal and opposite force resulting in the following:

*Note: The area over which the shear stress acts is equal to the width of the beam, **b**, multiplied by the length of the body, Δx.*

$$\Delta C = \tau b \Delta x \tag{25.6}$$

Equating Eqs. (25.5) and (25.6) and isolating for the shear stress results in the following:

$$\tau = \frac{\Delta M}{\Delta x}\frac{Q}{Ib} \tag{25.7}$$

If the length of our body approaches zero, then the term $\Delta M/\Delta x$ becomes equal to the shear force $\mathbf{V}$ due to Eq. (25.3), resulting in Jourawski's equation which is reproduced below:

$$\tau = \lim_{\Delta x \to 0} \frac{dM}{dx}\frac{Q}{Ib} = \frac{VQ}{Ib} \tag{25.8}$$

Calculating the First Moment of Area, Q

$\mathbf{Q}$ is defined as the first moment of area of the portion of the cross-sectional area about the centroidal axis of the member. The area considered is taken as the area from the depth of interest to the top or the member, or the area from the bottom of the member to the depth of interest, $\mathbf{y_A}$:

$$Q(y = y_A) = \int_{y_{bot}}^{y_A} y\,dA = \int_{y_A}^{y_{top}} y\,dA \tag{25.9}$$

Note: When calculating $\mathbf{Q}$, the area under consideration can be broken up into n smaller areas whose local centroid is easier to calculate. If this is done, then Eq. (25.10) becomes:

$$Q = \sum_{i=1}^{n} A_i d_i \tag{25.11}$$

$\mathbf{Q}$ can be evaluated by following the procedure outlined below:
  i.   Determine the depth of interest where $\mathbf{Q}$ is being calculated.
  ii.   Calculate the area, $\mathbf{A}$, of the cross section between the depth of interest to the top of the member; alternatively, the area of the cross section between the depth of interest to the bottom of the member.
  iii. Determine the distance between the centroid of the area found in step ii and the centroid of the cross section, $\mathbf{d}$.
  iv.   Calculate $\mathbf{Q}$ using Eq. (25.10):

$$Q = Ad \tag{25.10}$$

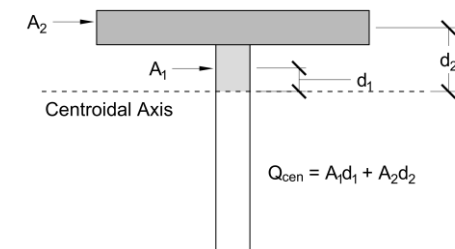*Fig. 25.6 shows the application of Eq. (25.11) to find the shear stress at the mid-height of a T-beam*

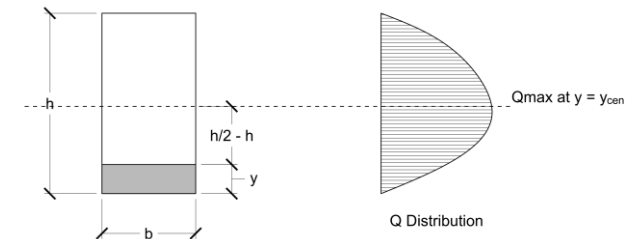Fig. 25.6 – Calculating Q for more complex shapes

Distribution of Shear Stresses

Like the axial stresses caused by bending moments, the shear stresses carried in a member are not constant over the depth of the cross section. This is because $\mathbf{Q}$ depends where the shear stress is being calculated, and the width of the member, $\mathbf{b}$, may vary over the height of the member.

Consider a rectangular cross section, shown in Fig. 25.7, which has a height of $\mathbf{h}$, a width of $\mathbf{b}$, and whose centroidal axis is located at a height of $\mathbf{h/2}$ above the base. The value of $\mathbf{Q}$ calculated for an arbitrary depth located a distance $\mathbf{y}$ from the bottom of the cross section is:

$$Q = Ad = (by) \times \left(\frac{h}{2} - \frac{y}{2}\right) = \frac{1}{2}by(h - y) \tag{25.11}$$

From Eq. (25.11), we can deduce three properties of $\mathbf{Q}$ which generally apply to all cross-sectional shapes:
  i. $\mathbf{Q}$ varies parabolically over the height of the member
  ii. $\mathbf{Q}$ is equal to 0 at $y = 0$ and $y = h$, i.e. $\mathbf{Q}$ is equal to zero at the top and the bottom of the member
  iii. The largest value of $\mathbf{Q}$ occurs at $y = h/2$. In general, $\mathbf{Q}$ is maximized at the centroidal axis of the member

For rectangular members, $\mathbf{b}$ is a constant, and hence the shear stress distribution will be parabolic.

Fig. 25.7 – Derivation of Q for a rectangular cross section and resulting distribution over the member height.

Lecture 26 – Wood Beams

Overview:

Along with steel and concrete, wood is one of the most commonly used materials for building structures. In this chapter, the various structural properties of wood are discussed, and tables of wood properties are presented and explained.

Properties of Wood

Wood has historically been used as a building material since perhaps the beginning of civilization due to its strength, workability, and abundance in nature in many parts of the world. Woods can be classified as being *softwoods* or *hardwoods*, with softwoods typically coming from coniferous trees and the hardwoods from deciduous species. Hardwoods are typically stronger, stiffer, heavier, and more difficult to work with than softwoods. Due to their relatively low cost and ease of use, softwoods tend to be used extensively in construction, while the more expensive hardwoods tend to be used for furniture, high-end finishes and musical instruments due to their durability. Examples of softwood and hardwood species are shown in Fig. 26.1.

1.11 Softwoods and Hardwoods

Figure 1.11 shows two small blocks of wood highly magnified. It is noticeable that these two pieces differ considerably in their cell structures. They have been chosen as representing two distinct classes into which practically all timbers can be divided.

Fig. 1.11.—Diagrammatic representation of a block of (a) hardwood and (b) softwood showing the major characteristic features. Note the large pores present in (a) but absent in (b).

Fig. 26.2 – Schematic showing the structure of hardwoods (left) and softwoods (right).
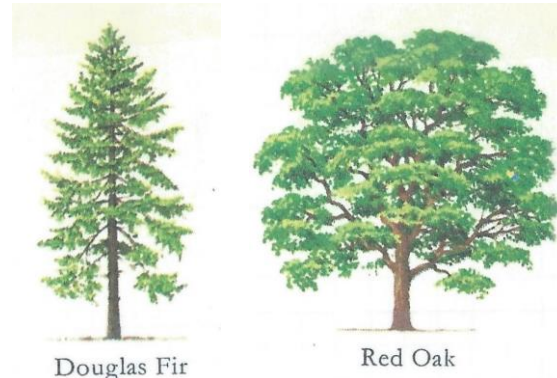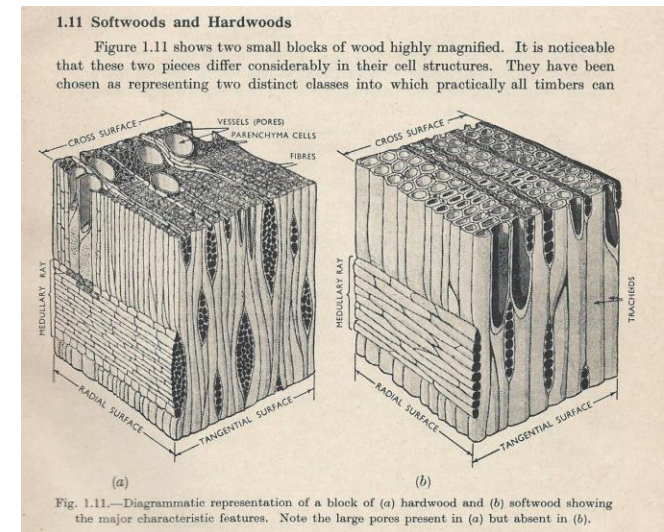

Fig. 26.1 – Examples of a softwood (Douglas Fir) and a hardwood (Red Oak)

The internal structures of both types of woods, shown in Fig. 26.2, resemble a series of fibres oriented along the height of a growing tree. Within the hardwood, there is a mixture of larger vessels embedded in a tightly-packed matrix of smaller fibres, while the softwoods are composed of uniformly distributed vessels which are hollow to allow water and nutrients to move throughout the tree. The dense fibres in the hardwood give the material its strength, stiffness and weight, while the relatively soft tubes in the softwood make it easier to work with.

Wood, being a naturally occurring material, differs in many ways from an engineered material like steel. Since the structure of wood is biased along the height of the tree, the material properties of wood are different depending on direction of loading relative to the orientation of the fibres; this is unlike the uniform response which steel exhibits. The property of having different mechanical properties in various directions makes wood an *anisotropic* material, unlike steel which is an *isotropic* material.

*Note: The strength and stiffness of wood generally differ parallel to the grain and perpendicular to the grain; because these directions are orthogonal, wood is example of an **orthotropic** material, which is a subset of anisotropic materials.*

Another important aspect to consider when working with timber structures is that wood has a wide range of mechanical properties which cannot be precisely specified in design. Therefore, appropriate values of strength and stiffness to use in design must be obtained by extensive testing, and larger factors of safety are typically employed.

Response of Wood to Loading
Timber members, often used as beams or columns in structures, typically need to support axial loads, bending moments, and shear forces. Wooden members tend to perform well when loaded in ways which resemble the forces which trees must resist in nature, namely high bending moments and axial forces which act along the direction of the fibres. When subjected to axial forces which act parallel to the grain, wooden members are strong and stiff. This allows them to carry high tensile forces, which occur in a wooden truss structures, and high compression forces, which occur in columns in buildings.

In construction, large heavy objects are often placed on the ground and supported from below by smaller wooden pieces. This loads the wood in compression perpendicular to the grain. Under this loading condition, the response of the wood is much softer and ductile than when loaded parallel to the grain, especially in softwoods. This property makes wood an ideal material to use when placing delicate objects on the ground. The differences in the compression response of woods when loaded parallel to the grain and perpendicular to the grain is illustrated in Fig. 26.3.
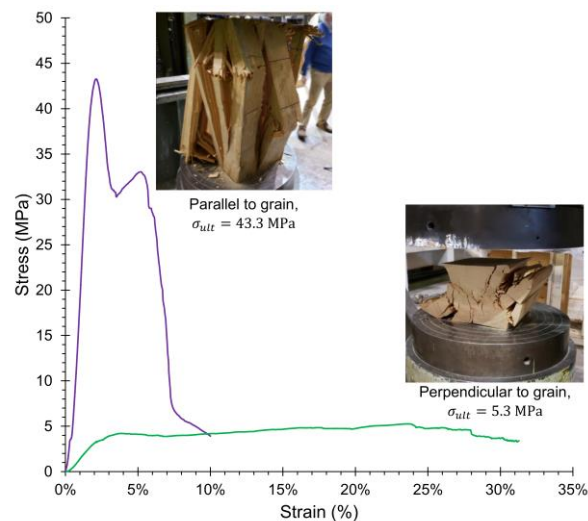

Fig. 6.3 – Comparison of stress-strain response of wooden members loaded in compression parallel to the grain and perpendicular to the grain.

When used in beams, timber members must carry significant bending moments and shear forces. Wooden members are strong in bending because the resulting flexural stresses act along the fibres of the material. However, they are susceptible to failing in shear because the fibres are can be separated by the resulting shear stresses relatively easily. An example of a wooden beam failing in shear can be seen in Fig. 26.4.

Fig. 26.4 – Timber beam loaded under four-point bending. Note the shear failure on the left side of the beam which has caused the previously vertical lines to separate, and the flexural failure at the midspan

Wood Design Tables

As noted earlier in the chapter, wood is not an engineering product and hence has great variability in its material properties. Fig. 26.5, which shows the failure stresses of 2110 small wooden specimens when loaded in flexure, illustrates the range of strengths which may exist even for specimens cut from the same tree. The measured strengths, which are roughly normally distributed, were on average 50.2 MPa. However, the weakest specimens were less than half of the average strength, and the strongest ones were approximately 60% stronger. **To account for the variability in strength, the 5th percentile strength is typically used in design, along with a factor of safety of 1.5.**
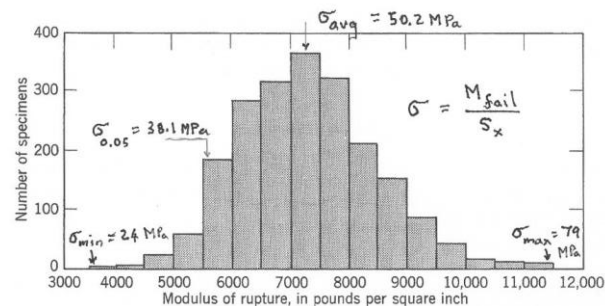
(b) Frequency distribution of bending strength of green Douglas fir. 2110 small clear specimens cut from a single tree. Short-term loading.

Fig. 26.5 – Distribution of flexural strengths obtained by testing 2110 small wooden specimens

Tables of material properties of many types of wood are shown in Table 26.1 and in Appendix D. The tables are categorized as being for smaller members (top) and for larger members (bottom). This is because the material strengths used in design vary depending on the size of the wooden members used. Smaller members tend to be weaker on average because they are more strongly influenced by the presence of knots and other defects in the material.

In the tables, the 5th percentile Young's modulus, E_{05}, and the average Young's modulus, E_{50}, are provided in the far-right columns. When determining the strength of a member, like when estimating its buckling load, E_{05} should be used. Deflection calculations on the other hand should be done using E_{50}.

Table 26.1 – Wood Properties. Small specimens (top) and large specimens (bottom)

Section 9	Wood Structures

5th Percentile estimates of strength under one month loading. For safe working stresses reduce these breaking stresses by factor of safety of 1.5. Page 259

9 – 11.2 (a)   Specified strength and modulus of elasticity for dimension lumber, thickness 38 to 77 mm, MPa**

Species or Species Combination	Grade	Bending f_{bu}	Shear Longitudinal f_{vu}	Compression Parallel to Grain f_{pu}	Compression Perpendicular to Grain f_{qu}	Tension Parallel to Grain f_{tu}	Modulus of Elasticity E_{50}	Modulus of Elasticity E_{05}
Douglas Fir-Larch	Select Structural	17.5	1.1	16.5	3.6	13.5	11,000	8,000
	No. 1 and No. 2	10.0	1.1	9.0	3.6	9.0	9,500	6,000
Hem-Fir	Select Structural	16.0	0.8	14.5	1.9	13.5	11,000	7,500
	No. 1 and No. 2	11.5	0.8	10.5	1.9	9.0	10,500	7,000
Lodgepole Pine, or Ponderosa Pine	Select Structural	16.0	1.0	14.5	1.9	13.5	10,000	7,000
	No. 1 and No 2	11.5	1.0	10.5	1.9	9.0	9,000	6,000
Jack Pine	Select Structural	16.0	1.0	14.5	2.6	13.5	10,500	7,000
	No. 1 and No. 2	11.5	1.0	10.5	2.6	9.0	9,500	6,000
Red Pine	Select Structural	11.5	0.8	10.0	1.9	10.0	7,000	5,000
	No. 1 and No. 2	8.0	0.8	7.0	1.9	7.0	6,000	4,000
White Pine*	Select Structural	6.0	0.8	–	1.9	–	5,500	4,000
	No. 1 and No. 2	4.5	0.8	–	1.9	–	4,500	3,500

*   For use in stress-laminated decks only.
**   Dimension lumber with thickness of 89 mm or greater shall have specified strengths in accordance with Table 13–11.2 (b).

9 – 11.2 (b)   Specified strength and modulus of elasticity for beams & stringers, post & timbers, minimum dimension 140 mm, MPa

Species or Species Combination	Grade	Bending f_{bu}	Shear Longitudinal f_{vu}	Compression Parallel to Grain f_{pu}	Compression Perpendicular to Grain f_{qu}	Tension Parallel to Grain f_{tu}	Modulus of Elasticity E_{50}	Modulus of Elasticity E_{05}
Douglas Fir-Larch	Select Structural	24.0	1.1	16.5	3.6	13.0	11,000	7,500
	No. 1	20.0	1.1	9.0	3.6	9.0	9,500	6,500
Hem-Fir	Select Structural	20.0	0.8	14.5	1.9	13.0	11,000	7,500
	No. 1	18.0	0.8	10.5	1.9	9.0	10,500	7,000
Lodgepole Pine, or Ponderosa Pine	Select Structural	18.5	1.0	14.5	1.9	13.0	10,000	7,000
	No. 1	13.0	1.0	10.5	1.9	9.0	9,000	6,000
Jack Pine	Select Structural	18.5	1.0	14.5	2.6	13.0	10,500	7,000
	No. 1	13.0	1.0	10.5	2.6	9.0	9,500	6,000
Red Pine	Select Structural	13.0	0.8	10.0	1.9	10.0	7,000	5,000
	No. 1	9.0	0.8	7.0	1.9	7.0	6,000	4,000

Lecture 27 – Shear Stresses in I Beams and Box Beams

Overview:
In this lecture, procedures for calculating the shear stresses for more complex shapes are discussed.

Shear Stresses in Complex Shapes:
For a member with second moment of area **I** and subjected to a shear force **V**, Jourawski's equation can be used to determine the shear stresses, τ:

$$\tau = \frac{VQ}{Ib} \tag{27.1}$$

When Eq. 27.1 was used to find the shear stresses for a rectangular member in Lecture 25, **b** was constant over the height and the change in shear stresses over the height was due to the varying first moment of area, **Q**, defined as:

$$Q(y = y_A) = \int_{y_{bot}}^{y_A} y\,dA = \int_{y_A}^{y_{top}} y\,dA \tag{27.2}$$

*Note: Recall that **Q** can be calculated by integrating from the bottom of the member up to the depth of interest, or by integrating from the top of the member down to the depth of interest. Both will produce the same result; this is reflected in Eq. 27.2.*

In Eq. (27.2), y_A is the depth of interest, y_{bot} and y_{top} refer to the bottom and top of the cross section respectively, and **y** is the vertical distance measured from the centroid of the cross section. For complex shapes, **Q** is typically calculated by subdividing the area of interest into **n** smaller areas, A_I, whose centroids are each a distance d_i away from the centroid of the cross section. **Q** is then calculated as:

$$Q = \sum_{i=1}^{n} A_i d_i \tag{27.3}$$

When calculating the shear stresses in more complex shapes like I beams, T beams or box beams, Eqs. (27.1) to (27.3) are still valid. However, **Q** must account for the geometry more carefully and **b** is the width of the cross section at the location of interest. Fig. 27.1 illustrates an example of how **Q** and **b** are obtained when calculating the shear stresses in the web of an I beam.
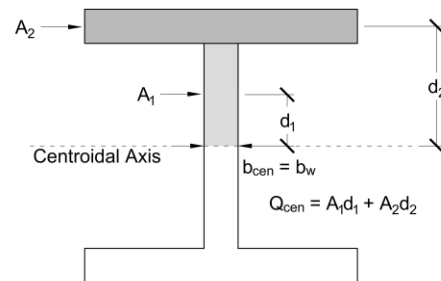

Fig. 27.1 – Calculation of shear stresses in an I beam

Built-Up Sections with Glued Components

It is common to construct larger cross sections by fastening together smaller components together using glue or mechanical fasteners like screws or nails. For these built-up sections, the ability of these connections to resist shear stresses is crucial for the section to behave together as a whole instead of several smaller pieces.

Note: The methods described in Figs. 27.2 and 27.3 can be used together when determining the shear stresses on glued surfaces with both horizontal and vertical components.
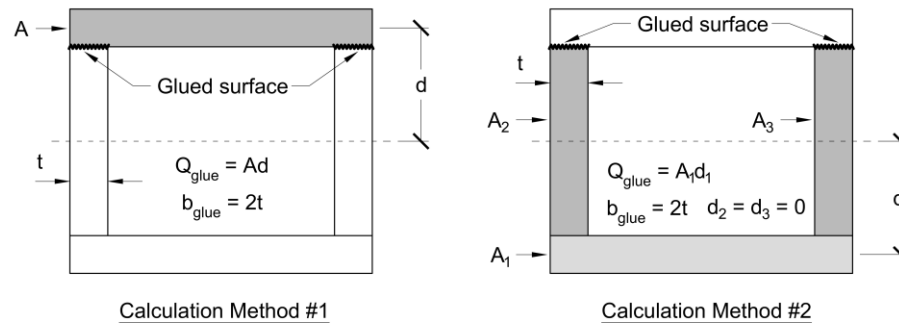
Fig. 27.2 – Calculating shear stresses for built-up sections with horizontal glued surfaces.
Either method will produce the correct value.

For horizontal glued surfaces, like those shown in Fig. 27.2, determining the shear stresses simply involves using Jourawski's equation at the depth of interest and taking **b** as the combined width of the interfacing surfaces. When the surfaces are vertical, like in the situations shown in Fig. 27.3, the typical procedure for calculating **Q** still applies, however the value of **b** to use is the total width of the vertical glued surfaces. In this case, the area of interest in the calculation of **A** is now best described as the area of the cross section which will slide of the glue fails.
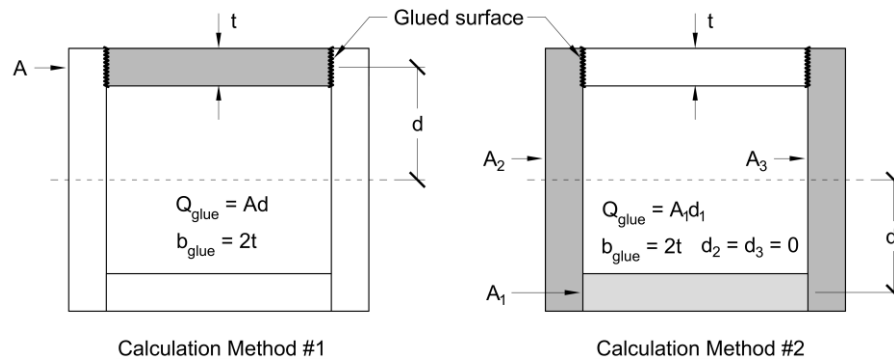
Fig. 27.3 – Calculating shear stresses for built-up sections with vertical glued surfaces
Either method will produce the correct value.

Distribution of Shear Stresses

Having a variable width over the height of a member has a pronounced effect on the shear stress distribution. For these shapes, **Q** is still equal to zero at the top and bottom of the member, reaches its maximum at the centroid, and varies parabolically in between. Applying Jourawski's equation results in the somewhat unusual shear stress distributions shown in Fig. 27.4. The shear stress distribution largely follows the shape of **Q**, but suddenly increases when there is an abrupt reduction in width, and suddenly decreases for abrupt increases in width.

Note: When determining the maximum shear stress in a member with varying width, a good strategy is to check both the narrowest part of the member and at the centroidal axis.

Jump due to change in width

Cross Section   First Moment of Area, Q   Shear Stresses, τ
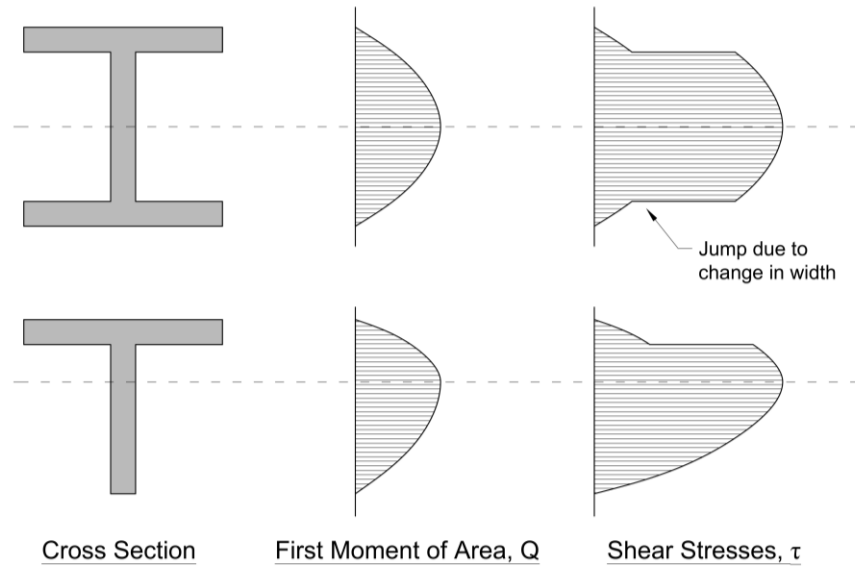
Fig. 27.4 – Shear stress distributions for a wide flange (top) and T-shaped (bottom) sections

Lecture 28 – Thin-Walled Box Girders

Overview:
Hollow structures are efficient, being lightweight yet strong and stiff. In this chapter, the development and use of hollow members made from assemblies of thin plates is discussed.

Advantages of Hollow Structures
The obvious advantage of using hollow members is that they weigh less than solid members which share the same outside dimensions. This reduction in weight however does not coincide with an equivalent reduction in strength and stiffness. Consider a hollow square member which has outside dimensions **b**, and thickness **t**. Its cross-sectional area, which is related to its weight, is equal to:

$$A = b^2 - (b - 2t)^2 \tag{28.1}$$

The second moment of area, **I**, which is related to the member's flexural stiffness and buckling strength, is equal to:

$$I = \frac{b^4}{12} - \frac{(b - 2t)^4}{12} \tag{28.2}$$

Eqs. (28.1) and (28.2) show that **A** and **I** do not decrease at the same rate as a solid member gradually becomes hollow; in the case of the area, it reduces quadratically while the second moment of area follows a quartic relationship. These relationships are plotted in Fig. 28.1.
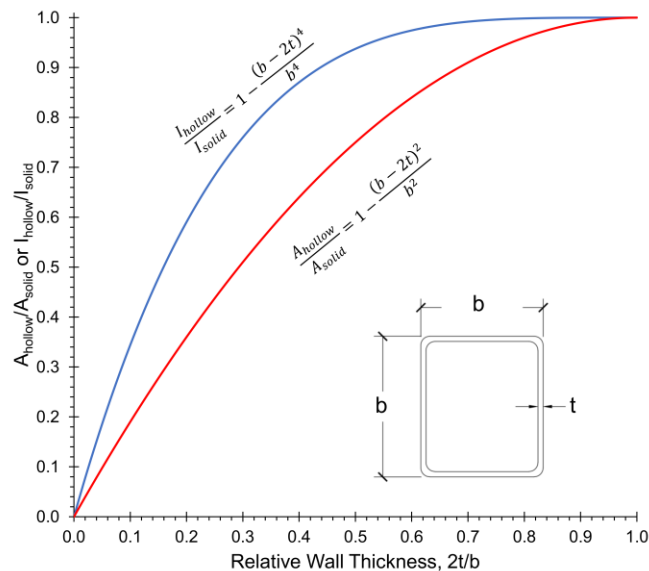
Fig. 28.1 – Relationship between A (red) and I (blue) and the wall thickness of a hollow square member.

As shown in Fig. 28.1, reducing the area, and hence the weight, of members by making them hollow leads to smaller reductions in the flexural stiffness. This makes hollow members useful for situations where the bending stiffness is important, like in beams or slender columns which tend to fail by buckling.

Design Considerations
In many ways, thin-walled hollow structures behave in the same way as solid members: they may fail by yielding in tension, buckling is a possibility when in compression, and they may also fail due to high flexural or shear stresses. An additional consideration for hollow members is that they may also fail due to *local buckling* of the thin walls. This kind of buckling is characterized by an instability of the walls themselves, as opposed to instability of the complete member, which is the case with Euler buckling. Thin plate buckling is discussed in more detail in Lectures 29 and 30.

Historical Development
A significant advance in the use of thin-walled box girders was in the Brittania Bridge, which was designed by the English engineer Robert Stevenson and built between 1847 and 1850. Stevenson's bridge, shown under construction in Fig. 28.2, consisted of two iron tubes running side by side over a clear span of 460 ft. This was a significant engineering accomplishment because the previous record for the longest box girder was only 31 ft.

The elevation, plan, and cross section views of the bridge are shown in Fig. 28.3. The structure ran continuously over several intermediate supports, being subjected to both large positive and negative bending moments along its full span. In regions of positive moments, which typically occurred between the supports, the top of the bridge carried flexural compression stresses. The negative moment regions occurred over the supports, and typically resulted in slightly smaller compressive stresses which instead acted on the bottom of the member. To prevent the thin plates on the top and bottom of the bridge from locally buckling, Stevenson had vertical stiffeners fastened to them, restraining them from moving up and down. These stiffeners, which are visible in the cross section of the bridge, were more closely spaced on the top flange because the flexural compression stresses were higher in these areas.
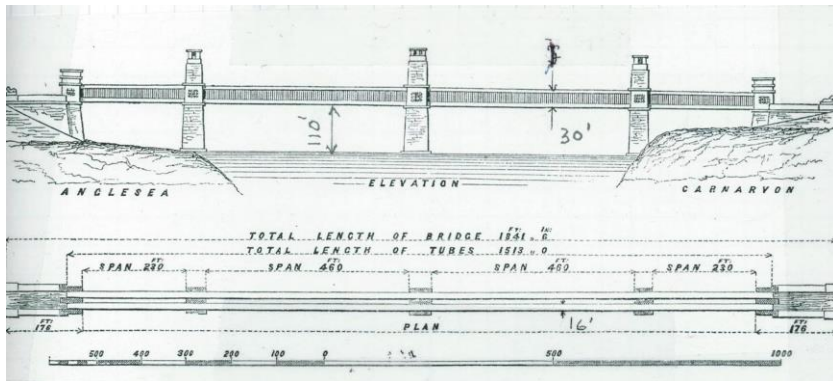

Fig. 28.2 – The Brittania Bridge under construction

Fig. 28.3 – Elevation (top left), plan (bottom left) and cross section (right) views of the Brittania Bridge

Fig. 28.4 – Surviving segment of the original Brittania Bridge

Lecture 29 – Buckling of Thin Plates

Overview:
Buckling of thin plates is a phenomenon which occurs in thin-walled sections which are subjected to axial compression, moment, or shear. In this chapter, the basic equations for characterizing the strength of plates are presented for common cases.

Theoretical Background:
In Lecture 14, the derivation of Euler's equation for slender members was presented. Euler's equation, which is applicable for one-dimensional members with length **L** and flexural stiffness **EI**, states that the buckling load for a member free to rotate on its two ends is:

$$P_e = \frac{pi^2 EI}{L^2} \tag{29.1}$$

For a plate which has a width of **b** and thickness **t** like the one shown in Fig. 29.1, the second moment of area will be equal bt³/12. Substituting this into Eq. (29.1) and rearranging terms results in the following equation for the buckling stress, **σ_crit**:

$$\sigma_{crit} = \frac{\pi^2 E}{12}\left(\frac{t}{L}\right)^2 \tag{29.2}$$

Fig. 29.1 – Rectangular plate loaded in compression with no restraints on the sides

Consider the plate which is shown in Fig. 29.2 which is subjected to a horizontal compression stress which acts along its left and right faces. In addition to the restraints on its two horizontal edges, the two vertical sides of the plate are restrained from moving in the out-of-plane direction. For this scenario, if the width of the plate, **b**, is larger than its unrestrained length **L**, then the required stress to buckle the plate is equal to the following:

$$\sigma_{crit} = \frac{k\pi^2 E}{12(1-\mu^2)}\left(\frac{t}{b}\right)^2 \tag{29.3}$$

Eq. (29.3) is the solution to a fourth order partial differential equation for the displaced shape of a thin plate subjected to compressive stresses. This equation, whose solution was formulated by the American-Russian-Ukrainian engineer Stephen Timoshenko, is a two-dimensional extension of Euler's equation for slender one-dimension members buckling under compressive loads. Although the derivation of the solution is beyond the scope of CIV102, the key idea is that **k** depends on the applied loading conditions (i.e. distribution of compressive stresses) and the boundary conditions (i.e. how the edges of the plate are restrained from moving).
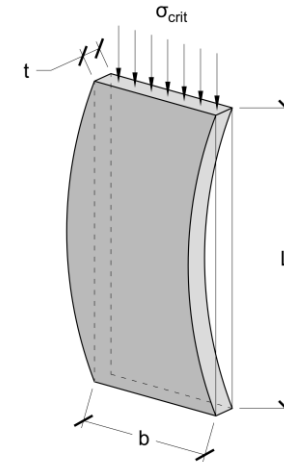
Note: μ is the Poisson's ratio of the material, which is a measure of how much a material deforms in the directions orthogonal to an applied load. For example, for a material which is being stressed in the x-direction, the transverse strain ε_y is equal to:

$$\varepsilon_y = -\mu\varepsilon_x = -\mu\frac{\sigma_x}{E} \tag{29.4}$$

Because the vertical surfaces are restrained from moving, ε_y is equal to zero. This means that an additional y-direction stress must be provided to make the net strain equal to zero:

$$\sigma_y = -\varepsilon_y E = \mu\sigma_x \tag{29.5}$$

This produces a carryover effect in the x-direction, reducing the longitudinal strain ε_x to be the following:

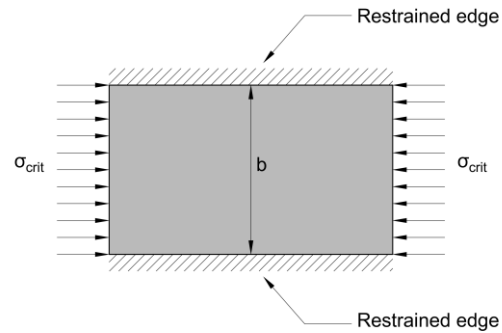$$\varepsilon_x = \frac{\sigma_x(1-\mu^2)}{E} \tag{29.6}$$

Fig. 29.2 – Rectangular plate loaded in compression and restrained along its two horizontal edges.

Plate Buckling Equations:
For the plate shown in Fig. 29.2 whose sides are restrained from movement both in and out of plane, the solution to the buckling coefficient **k** is the following equation:

$$k = \left(\frac{1}{n}\frac{L}{b} + n\frac{b}{L}\right)^2 \tag{29.7}$$

In Eq. (29.7), **n** is the number of half cycles which the buckled shape of the plate assumes, which is similar to Euler's solution for the buckled shape of one-dimensional struts. This equation is plotted in Fig. 29.3, and although it assumes a wide range of values for different values of L/b and n, the lowest possible value is k = 4. Therefore, a reasonable lower bound of the buckling stress which is appropriate for design is:

$$\sigma_{crit} = \frac{4\pi^2 E}{12(1-\mu^2)}\left(\frac{t}{b}\right)^2 \tag{29.8}$$

Fig. 29.4 shows a rectangular plate which is loaded with a constant compressive stress on its boundaries like the one shown Fig. 29.2. However, only one edge which is restrained from moving while the other edge is free to move. In this situation, the free edge greatly weakens the plate under compressive stresses, and it fails at a stress of:

$$\sigma_{crit} = \frac{0.425\pi^2 E}{12(1-\mu^2)}\left(\frac{t}{b}\right)^2 \tag{29.9}$$

This factor, (1-μ²), therefore appears in the plate buckling equation to account for the extra rigidity provided by the restrained edges and the Poisson effect.
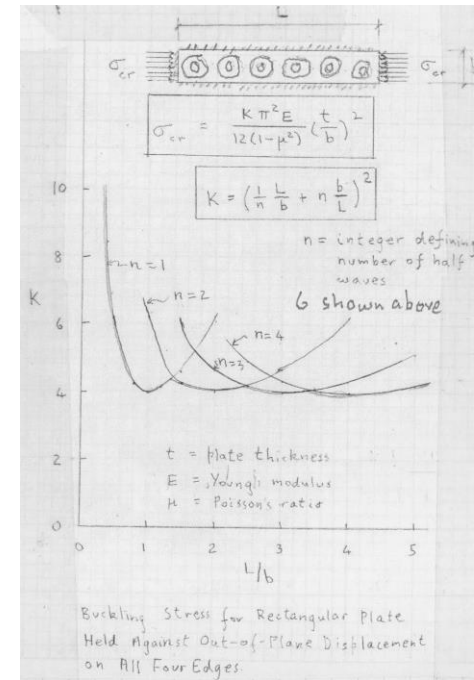

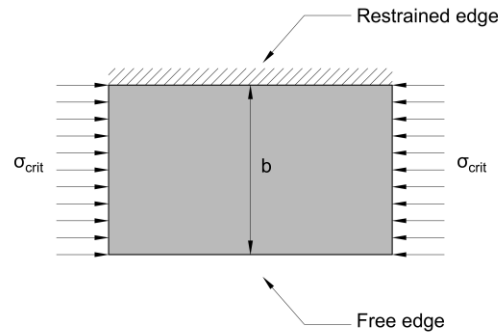Fig. 29.3 – Plot of k values for different L/b and n values

Fig. 29.4 - Rectangular plate loaded in compression with only one restrained horizontal edge

Fig. 29.5 show a rectangular plate which, unlike the ones shown in Figs. 29.2 and 29.4, carries compressive stresses which vary linearly from zero to a maximum on each side. The magnitude of the maximum stress which causes buckling is:

$$\sigma_{crit} = \frac{6\pi^2 E}{12(1-\mu^2)}\left(\frac{t}{b}\right)^2 \tag{29.10}$$

High shear stresses carried by thin plates can also cause buckling due to the diagonal compressive stresses which are caused by shear. The shear stress which causes a thin plate to buckle is:

$$\tau_{crit} = \frac{5\pi^2 E}{12(1-\mu^2)}\left(\left(\frac{t}{h}\right)^2 + \left(\frac{t}{a}\right)^2\right) \tag{29.11}$$

In Eq. (29.11), **h** is the height of the plate, and **a** is the spacing between vertical stiffeners which prevent the plate from moving in the out-of-plane direction. These terms are illustrated in Fig. 29.6.

Summary of Plate Buckling Equations
Fig. 29.7 contains a complete summary of the buckling stresses for the four situations discussed in Eqs. (29.8) to (29.11). The figure shows the various situations in which they can be used in the design of thin-walled box girder. The first two equations apply to the flange which is in compression due to the flexural compression. The compressive stresses from the moment may also cause the webs to buckle; the third equation can be used to predict when this might happen. Finally, the fourth equation should be used to determine if the shear stresses cause the webs to buckle. The application of these examples in design are discussed in more detail in Lecture 30.
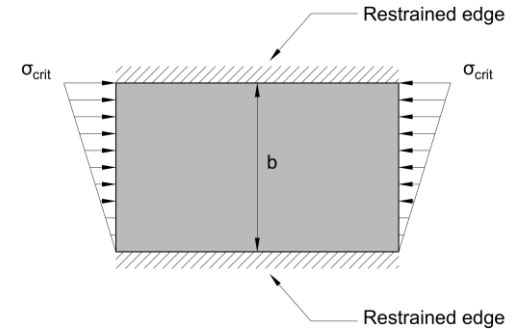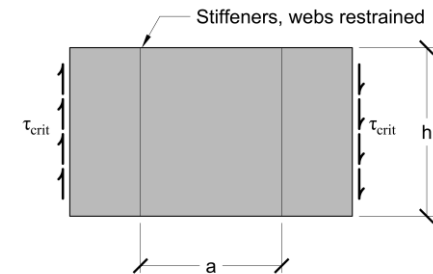

Fig. 29.5 - Rectangular plate loaded in compression and restrained on its two horizontal edges, but loaded with linearly varying compressive stresses

Fig. 29.6 - Rectangular plate subjected to shear stresses, with a height of h. The plate is restrained from buckling in the out-of-plane direction by vertical stiffeners which are spaced apart by a distance a.
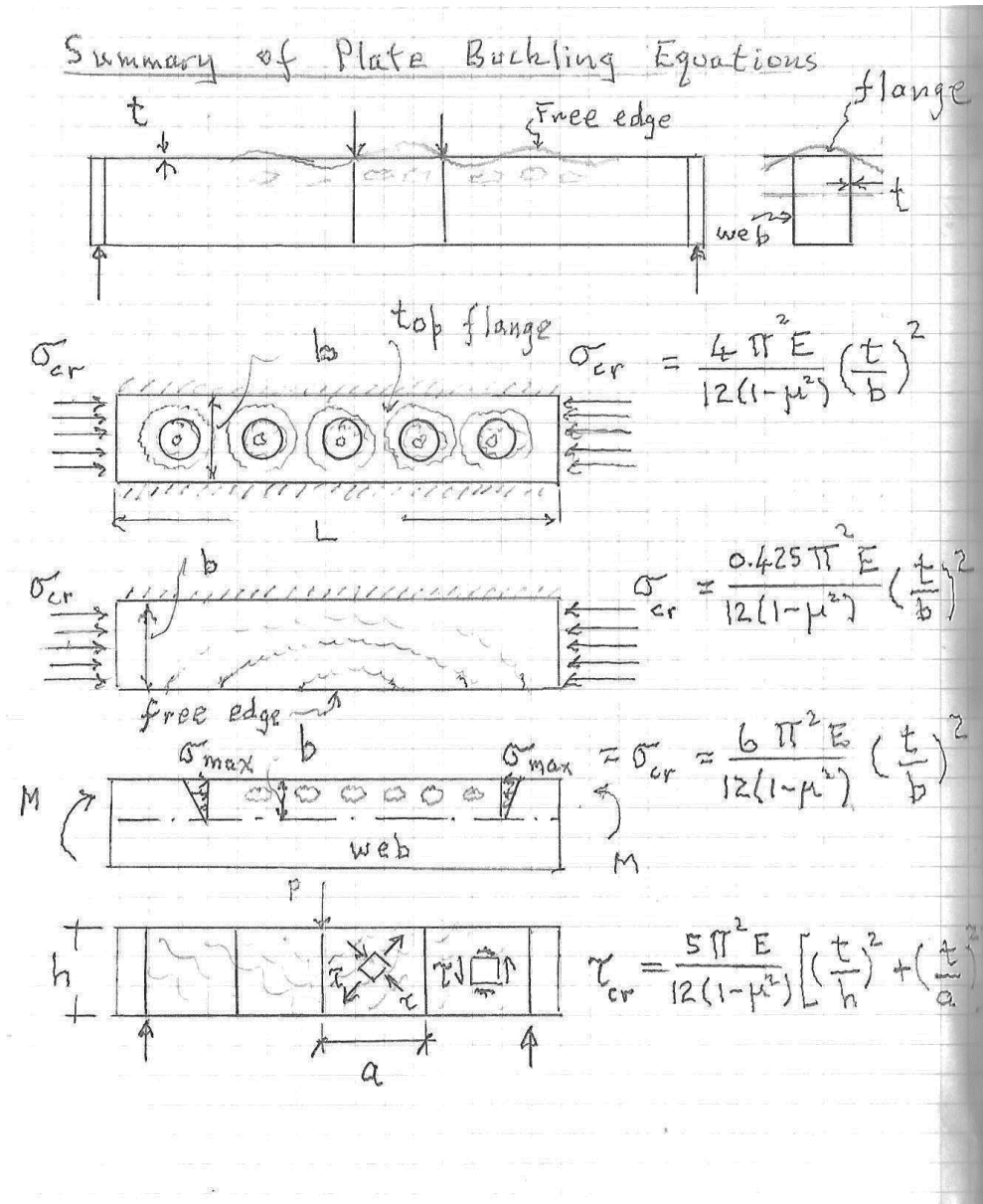
Fig. 29.7 – Summary of plate buckling equations used in the design
of a thin-walled box girder

Lecture 30 – Design of a Thin-Walled Box Girder

Overview:
In this chapter, the procedures described in this unit are summarized and applied to the design of a thin-walled box girder. Failures associated with both failure of the materials and buckling the thin plates are considered.

Basic Design Considerations
Consider the simply supported thin-walled box girder shown in Fig. 30.1 which is subjected to a single point load at its midspan. It is subjected to a constant shear force over its entire length and bending moments which linearly increase to a maximum at the midspan.
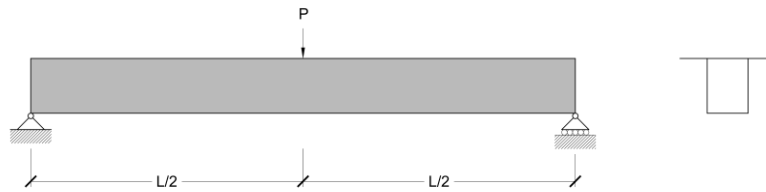

Fig. 30.1 – Example of a thin-walled box girder. Elevation (left) and cross section (right) views

If the tensile strength of the material, σ_{ult}^+, the compressive strength of the material, σ_{ult}^-, the shear strength of the material, τ_{ult}, and the shear strength of the material used to fasten the walls together, τ_m, are known, then there are four modes of material failure which are summarized in Table 30.1.

Note: Some examples of fastening materials include glue, screws, bolts or nails.

The design of thin-walled structures must also consider the possibility of buckling of the walls. Recall from Lecture 15 that when a structure is subjected to compressive stresses, it will fail at the lower of the ultimate compressive stress or the critical buckling stress:

$$\sigma_{fail} = \min\{\sigma_{ult}^-, \sigma_{crit}\} \tag{30.1}$$

When designing struts for compression, we used the critical buckling stress, σ_{crit}, as the Euler buckling stress. For the two-dimensional plates which make up the walls of a thin-walled box girder, σ_{crit} is instead taken as the appropriate plate buckling equation from Lecture 29.

Table 30.1 – Summary of material failure modes

No.	Failure Mode	Failure Condition	Relevant Design Equation
1	Tensile failure of walls	$\sigma = \sigma_{ult}^+$	$\sigma = \dfrac{My}{I}$
2	Compressive failure of walls	$\sigma = \sigma_{ult}^-$	
3	Shear failure of walls	$\tau = \tau_{ult}$	$\tau = \dfrac{VQ}{Ib}$
4	Shear failure of fastening material	$\tau = \tau_m$	

Table 30.2 – Summary of plate buckling failure modes

No.	Failure Mode	Failure Condition	Relevant Design Equation
5	Buckling of the compressive flange between the webs	$\sigma = \dfrac{4\pi^2 E}{12(1-\mu^2)}\left(\dfrac{t}{b}\right)^2$	
6	Buckling of the tips of the compressive flange	$\sigma = \dfrac{0.425\pi^2 E}{12(1-\mu^2)}\left(\dfrac{t}{b}\right)^2$	$\sigma = \dfrac{My}{I}$
7	Buckling of the webs due to the flexural stresses	$\sigma = \dfrac{6\pi^2 E}{12(1-\mu^2)}\left(\dfrac{t}{b}\right)^2$	
8	Shear buckling of the webs	$\tau = \dfrac{5\pi^2 E}{12(1-\mu^2)}\left(\left(\dfrac{t}{h}\right)^2 + \left(\dfrac{t}{a}\right)^2\right)$	$\tau = \dfrac{VQ}{Ib}$

As noted in Lecture 29, large shear stresses can cause also thin plates to buckle as well due to the resulting diagonal compressive stresses. Therefore, the walls will fail at the lower of the shear strength or the critical shear buckling stress:

$$\tau_{\text{fail}} = \min\{\tau_{ult}, \tau_{crit}\} \tag{30.2}$$

Including the additional buckling considerations results in the four more possible failure modes which must be considered in the design of the box girder, which are summarized in Table 30.2.

To illustrate the design process, we will try to determine the lowest value of P which causes our example bridge to fail. To do this, we will express the maximum shear force and bending moments in terms of **P** and substitute these relationships into the appropriate design equations:

$$V = \frac{P}{2} \tag{30.3}$$

$$M = \frac{PL}{4} \tag{30.4}$$

Flexural and Shear Strength
The most straightforward modes of failure are associated with tensile and compressive failures caused by flexure. Combining Navier's equation with Eq. (30.4) and noting the top of the girder is in compression and bottom of the girder is in tension results in the following values of **P** causing failure. Note that the subscripts on **P** correspond to the failure modes described in Tables 30.1 and 30.2.
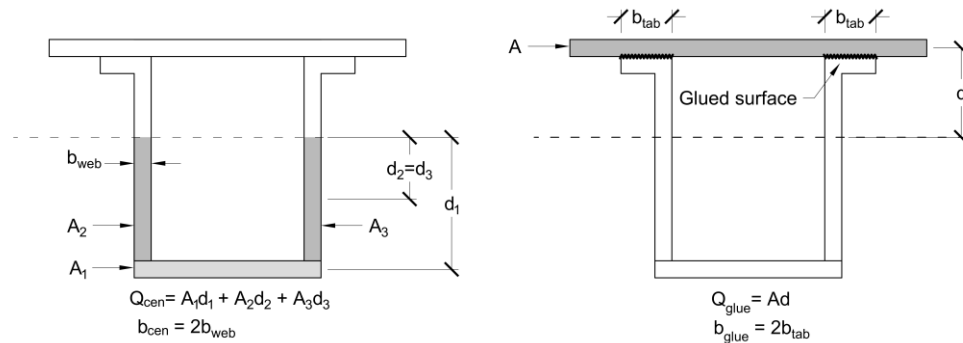
Fig. 30.2 – Calculation of Q to determine the shear stresses in the web (left) and in the glue (right)

$$\sigma_{ult}^{+} = \frac{\left(\frac{P_1 L}{4}\right) y_{bot}}{I} \rightarrow P_1 = 4\frac{\sigma_{ult}^{+} I}{L y_{bot}} \tag{30.5}$$

$$\sigma_{ult}^{-} = \frac{\left(\frac{P_2 L}{4}\right) y_{top}}{I} \rightarrow P_2 = 4\frac{\sigma_{ult}^{-} I}{L y_{top}} \tag{30.6}$$

The shear failures of the webs or the fastening material can be determined by using Jourawski's equation and calculating the appropriate values of **Q** and **b**. For the box girder being considered in this example, which is glued together, the areas and distances used to calculate **Q** and **b** are shown in Fig. 30.2. Using these values, the forces causing the shear failures of the web material and glue respectively are:

$$\tau_{ult} = \frac{\left(\frac{P_3}{2}\right) Q_{cen}}{I b_{cen}} \rightarrow P_3 = 2\frac{\tau_{ult} I b_{cen}}{Q_{cen}} \tag{30.7}$$

$$\tau_{m} = \frac{\left(\frac{P_4}{2}\right) Q_{glue}}{I b_{glue}} \rightarrow P_4 = 2\frac{\tau_{m} I b_{glue}}{Q_{glue}} \tag{30.8}$$

Failure Modes Associated with Plate Buckling

Calculating the loads which cause the structure to fail due to plate buckling is a matter of identifying which parts of the structure are carrying compressive (or shear) stresses, and then selecting the appropriate equation based on the distribution of these stresses and how the plate is restrained if applicable.
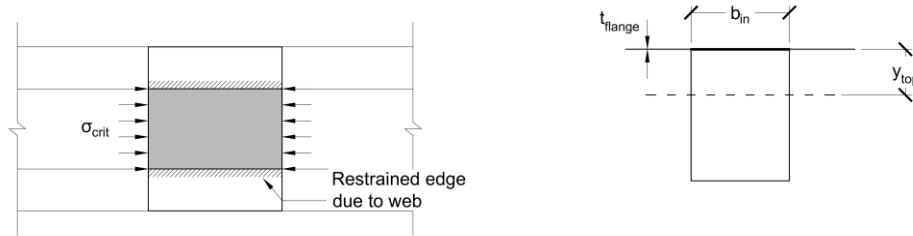
Fig. 30.3 – Buckling of the flange between the two webs. Top (left) and cross section (right) views.

Consider the region of the compression flange shown in Fig. 30.3 which is located between the two webs. Because the flange is located at constant height above the centroidal axis, the flange experiences uniform compressive stresses along its width from the bending moment. The webs, which are securely fastened to the flange from below, provide a restraint which prevents the region between the webs to move up or down. These boundary conditions suggest that the plate buckling equation with a coefficient of **k = 4** is appropriate for determining when failure occurs. Therefore, failure of this region of the bridge takes place at the following load:

*Note: Recall that the compressive stresses caused by bending do not vary over the width of the member because they are only a function of the vertical distance from the centroidal axis, **y**.*

$$\frac{4\pi^2 E}{12(1-\mu^2)}\left(\frac{t_{\text{flange}}}{b_{in}}\right)^2 = \frac{\left(\frac{P_5 L}{4}\right)y_{top}}{I} \rightarrow P_5 = \frac{16\pi^2 EI}{12Ly_{top}(1-\mu^2)}\left(\frac{t_{\text{flange}}}{b_{in}}\right)^2 \qquad (30.9)$$
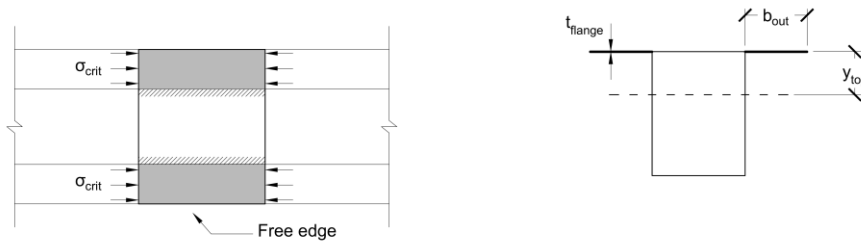

Fig. 30.4 – Buckling of the free edges of the flange. Top (left) and cross section (right) views.

The tips of the flange, shown in Fig. 30.4, may also buckle due to the flexural compressive stresses. Like the flange between the webs, they are also subjected to uniform stresses over their width. However, they have a free edge on one side which can move up or down, meaning the plate buckling equation with a coefficient of **k = 0.425** is more appropriate for determining their strength. Therefore, the load causing these tips to buckle, **P₆**, is equal to:

$$\frac{0.4254\pi^2 E}{12(1-\mu^2)}\left(\frac{t_{\text{flange}}}{b_{out}}\right)^2 = \frac{\left(\frac{P_6 L}{4}\right)y_{top}}{I} \rightarrow P_6 = \frac{1.7\pi^2 EI}{12Ly_{top}(1-\mu^2)}\left(\frac{t_{\text{flange}}}{b_{out}}\right)^2 \qquad (30.10)$$
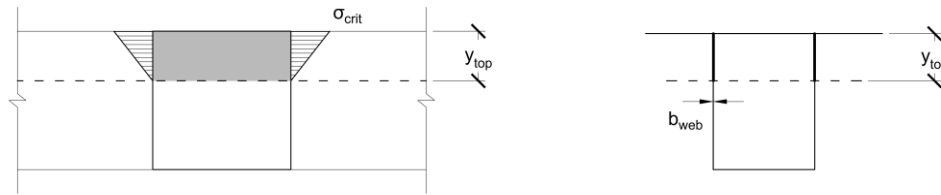
Fig. 30.5 – Buckling of the webs due to flexural compressive stresses. Side (left) and cross section (right) views.

The flexural compressive stresses can also cause the webs of the structure to buckle. These webs, which are oriented vertically, will experience compressive stresses which increases linearly from zero at the centroidal axis to a maximum at the top of the web. This linear gradient of stresses suggests that the plate buckling with the coefficient **k = 6** is the most appropriate. The load causing these webs to buckle, **P₇** (P_7), is therefore equal to:

$$\frac{6\pi^2 E}{12(1-\mu^2)}\left(\frac{b_{web}}{y_{top}}\right)^2 = \frac{\left(\frac{P_7 L}{4}\right)y_{top}}{I} \rightarrow P_7 = \frac{24\pi^2 EI}{12Ly_{top}(1-\mu^2)}\left(\frac{b_{web}}{y_{top}}\right)^2 \tag{30.11}$$

*Note: Even when there is more than one web in the structure, the width of **one** web is used in the plate buckling equations. This is because the equations are used to describe the strength of each individual plate which may buckle independently of each other.*

*Note: In Eq. 30.11, the value of **y** used to calculate the flexural stresses should be $y_{top} - t_{flange}$. If the thickness of the flange is small compared to y_{top}, then the following approximation is appropriate:*

$$t_{flange} \ll y_{top} \rightarrow y_{top} \approx y_{top} - t_{flange}$$
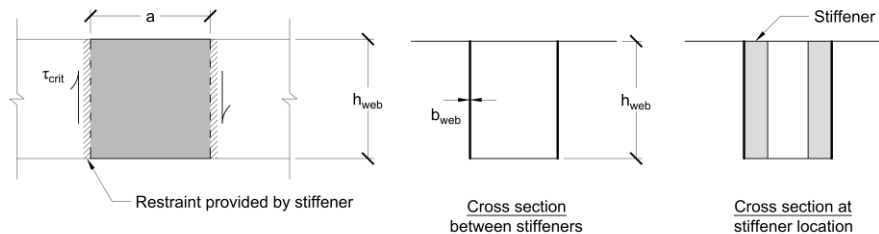

Fig. 30.6 – Buckling of the webs due to shear stresses. Side (left) and cross section (right) views.

Choosing the appropriate equation to determine when the webs buckle in shear is straightforward because only one of the four plate buckling equations is related to the shear stresses. Using Jourawski's equation and equating the critical shear buckling stress to the shear stresses in the web results in the following expression for **P₈** (P_8), where a is the spacing of stiffeners which restrain the web from moving side to side:

*Note: In design, appropriate factors of safety must be used to determine the lowest value of **P** which can be safely resisted by the structure.*

$$\frac{5\pi^2 E}{12(1-\mu^2)}\left(\left(\frac{b_{web}}{h_{web}}\right)^2 + \left(\frac{b_{web}}{a}\right)^2\right) = \frac{\left(\frac{P_8}{2}\right)Q_{cen}}{2Ib_{web}} \rightarrow P_8 = \frac{20\pi^2 EI}{12Q_{cen}(1-\mu^2)}\left(\left(\frac{1}{h_{web}}\right)^2 + \left(\frac{1}{a}\right)^2\right) \tag{30.12}$$

The strength of the structure is governed by the lowest value of **P** obtained from the eight calculations. Note that under more complex loading and support conditions, more calculations will be required to obtain the failure load.